

Rheinische Friedrich-Wilhelms-Universität Bonn
University Centre in Svalbard

Master Thesis in Meteorology

Snow Depth around Longyearbyen, Svalbard

submitted by

Antonia Louise Radlwimmer

Home Supervisor: Prof. Dr. Andreas Hense

Internal Supervisor: Dr. Siiri Wickström

January 31, 2023



ACKNOWLEDGMENT

Thank you to Siiri for all the help with models, matlab and carrying of ladders, logger boxes, instruments, masts and rocks. Thank you to Andreas for all the interest you took in this work despite already having retired. And thank you to my office and kitchen mates for providing a cheerful, comfortable space for all of this to happen.

CONTENTS

Abstract	i
Stakeholder Summary	iii
List of Abbreviations	v
List of Figures	viii
List of Tables	ix
1 INTRODUCTION	1
1.1 Motivation	1
1.2 Polar Meteorology	1
1.3 Svalbard	2
1.3.1 Research Site Svalbard	2
1.3.2 Precipitation on Svalbard	3
1.3.3 Precipitation on Svalbard in a Changing Climate	3
1.4 Observational Challenges	4
1.5 Research Questions	5
1.6 Outline	6
2 SNOW DEPTH OBSERVATIONS	9
2.1 Setup and Instrumentation	9
2.1.1 Setup	9
2.1.2 Instrumentation	10
2.2 Post-processing	13
2.2.1 Temperature Correction	13
2.2.2 Slope Correction	14
2.2.3 Unphysical Values	15
2.2.4 Resampling	15
2.3 Results	17
2.3.1 Processed Data Set	17
2.3.2 False Temperature Correction	17
2.3.3 Locality of Spatial Distribution as seen at Super Site	17
2.3.4 Representativeness of Observations of Snow Depths in Longyear- byen Area	19
2.3.5 Elements Evident in Temporal Evolution	19
2.4 Discussion and Summary	20
2.4.1 Spatial Distribution of Snow Depths in Longyeardalen	20
2.4.2 Temporal Evolution of Snow Depths in Longyeardalen	20
2.4.3 Summary	20
3 MODELLED SNOW DEPTHS	23

3.1	Description of the Model	23
3.2	Results	24
3.2.1	Results from Modelled Data	24
3.2.2	Comparison with Observations in the Spatial Dimension	26
3.2.3	Comparison with Observations in the Temporal Dimension	30
3.3	Discussion and Summary	33
4	SNOWFALL	35
4.1	Setup and Instrumentation	35
4.1.1	Setup	35
4.1.2	Precipitation Gauges	36
4.1.3	Optical Distrometer	36
4.2	Correction	37
4.2.1	Undercatch	37
4.2.2	Correction Models	38
4.3	Results	40
4.3.1	Results on the Correction Itself	41
4.3.2	Functional Relation between Corrected Precipitation and Snow Depth Difference	42
4.4	Discussion and Summary	43
5	WIND	47
5.1	Data	47
5.2	Results	48
5.2.1	Snow Depth Changes in Absence of Precipitation	48
5.2.2	Wind Speed Threshold for Wind Transport of Snow	49
5.2.3	Magnitude of Effect of Wind Transport of Snow	52
5.2.4	Prevailing Wind Directions	54
5.2.5	Changes in Snow Depths with Regard to Wind Directions	56
5.3	Discussion and Summary	61
5.3.1	Threshold Wind Speed for Snow Transport	61
5.3.2	Characteristics of Snow Transport	61
5.3.3	Directional Influence of Wind	61
6	CONCLUSION AND OUTLOOK	63
6.1	Fieldwork and Experimental Results	63
6.1.1	Processing Applied to Observations	63
6.1.2	Limits of Observations and Model	64
6.2	Precipitation's and Wind's Influence on Snow Depth Changes	65
6.3	Outlook	66

ABSTRACT

During the spring snow season of 2022, snow depths and the meteorological dependencies of their changes were investigated in the Longyearbyen area. The data set, comprising of in situ point observations and model data from SeNorge snow model, was found to represent the temporal evolution of snow depths in timing but not in magnitude. Spatial representativeness for the Longyearbyen area was not achieved by either observations or model. Both precipitation and wind were found to have great effect on the snow depth, but were dismissed as case to case proxies for changes in the snow depth.

STAKEHOLDER SUMMARY

In this study the snow depth distribution, evolution and dependency on meteorological parameters (precipitation and wind) was investigated for the Longyearbyen area. Instantaneous monitoring of snow accumulation on the avalanche-prone slopes around Longyearbyen is in place and has been operational since 2019 in the DRIVA project¹. But linking these observations to the local weather and climate system and existing meteorological knowledge on climate change will help inform snow depth expectations for the immediate and longer term future.

The snow depth data set, gathered in the spring snow season of 2022 and comprising of in situ point observations and model data from SeNorge snow model, was found to represent the temporal evolution of snow depths in timing but not in magnitude. Spatial representativeness for the Longyearbyen area was not achieved by either observations or model. Both precipitation and wind were found to have great effect on the snow depth, but were dismissed as case to case proxies for changes in the snow depth.

For the linking of snow depth behaviour and meteorological knowledge, an approach to snow depth monitoring with greater spatial coverage and continuity, e.g. lidar scanning, is recommended, to enhance representativeness of the observations.

¹<https://www.unis.no/arctic-safety-centre/driva>

LIST OF ABBREVIATIONS

SDD snow depth difference

SWE snow water equivalent

LIST OF FIGURES

Figure 1	Map of Svalbard Region	3
Figure 2	Satellite Image Map of Observation Sites	12
Figure 3	Schematic for Slope Correction	15
Figure 4	Snow Depth Observations, shown for Various Processing Steps	16
Figure 5	Photo of Snow Drift at Super Site	18
Figure 6	Snow Depth Observations Stacked with Weather Parameters from MetNorway Stations	21
Figure 7	Schematic Explaining Snow Depth Evolution in SeNorge Model	24
Figure 8	Map of SeNorge Mean Season Snow Depth, Svalbard	25
Figure 9	Map of SeNorge Elevations, Svalbard	25
Figure 10	Histogram of SeNorge's Snow Depths and Elevations, Svalbard	25
Figure 11	Map of SeNorge Mean Season Snow Depth, Longyearbyen	26
Figure 12	Map of SeNorge Elevations, Longyearbyen	26
Figure 13	Comparison of In Situ Snow Depth Observations and Modelled Snow Depths at Nearest SeNorge Grid Point	27
Figure 14	Elevations of SeNorge Grid Points and Observation Sites	28
Figure 15	Comparison of In Situ Snow Depth Observations and Modelled Snow Depths by Elevation Bin	29
Figure 16	Comparison of Mean of In Situ Snow Depth Observations and Mean of Modelled Snow Depths in the Longyearbyen Area	31
Figure 17	Photo Weather Station at Airport	36
Figure 18	Schematic of Different Gauge Shapes and their Performance Concerning Aerodynamic Blockage	37
Figure 19	Comparison of Undercatch Correction Models	40
Figure 20	Coefficients of Correction Factor for Undercatch	41
Figure 21	Scatterplot of Precipitation and Snow Depth Changes	44
Figure 22	Scatterplot of Precipitation and Snow Depth Changes for Low Wind	45
Figure 23	Wind from MetNorway, Super Site and AROME	48
Figure 24	Scatterplot of Wind Speed and Snow Depth Difference, only Cases Without Precipitation	50

Figure 25	Scatterplot of Difference of Wind Speed from Saltation Threshold and Snow Depth Difference, only Cases Without Precipitation	51
Figure 26	Histogram of Wind Speeds in the Event of Drifting Snow	52
Figure 27	Drifting Snow Fluxes and Wind Speeds	53
Figure 28	Prevalence of Wind Directions and Wind Speeds	55
Figure 29	Wind Rose with According Snow Depth Difference at SNOdar	56
Figure 30	Scatterplot of Wind Directions with According Snow Depth Differences	58
Figure 31	Wind Rose with According Snow Depth Change Frequencies	59

LIST OF TABLES

Table 1	Measuring Gaps at Super Site	10
Table 2	Snow Depth Observation Sites	11
Table 3	Snow Depth Data Sanity Mask	15
Table 4	Coefficients of Precipitation Correction Model Førland	39
Table 5	Coefficients of Precipitation Correction Model Rubel Hantel	39
Table 6	Snow Depth Differences Categorized by Presence of Precipitation	49
Table 7	Snow Depth Differences by Luv and Lee	60

INTRODUCTION

1.1 MOTIVATION

The ArctRisk project (*Risk governance of climate-related systemic risk in the Arctic*)¹, of which this master thesis is a part, aims to prepare northerly communities for coping with climate change and a shifting natural environment. The Arctic offers an involuntary pilot study, as climate warming has already progressed here farther and more rapidly than anywhere else in the world [20]. For the community of Longyearbyen, on the polar archipelago of Svalbard, precipitation related natural hazards such as snow or slush avalanches are prime objects of risk avoidance and mitigation.

Precipitation induced phenomena, including snow avalanches, slush avalanches and rain on snow events have caused loss of life and serious damage to infrastructure and economy in Longyearbyen in recent years ([7], [13], [11], [6]). They are associated with extreme weather events expected to occur more frequently with progressing climate change [12]. It is therefore vital to build a knowledge base for the behaviour of precipitation and, in particular, snow around Longyearbyen.

In this thesis, an experimental meteorological perspective is taken on snow in the Longyearbyen area. This perspective will add to the understanding of snow amounts, snow distributions and their meteorological dependencies in the region, linking meteorological knowledge on climate change to its practical implications in natural hazard management.

1.2 POLAR METEOROLOGY

Polar meteorology is subject to a unique set of circumstances, setting it apart from the meteorological paradigms of other latitudes. Meteorological patterns in the polar regions are shaped markedly by the extremes of polar night and day, by air-ice-sea interactions and the extent of land-fast or perennial sea ice [24].

¹<https://www.ntnu.edu/iot/arct-risk>

At the same time, polar regions are among the least observed places on Earth. The harshness of weather, the limited human population and the seclusion from human infrastructure have resulted in a relative lack of meteorological data spanning their vast spatial expanses. There have been recent advances in observation coverage connected to unmanned sites [14] or satellites and data coverage connected to data assimilation [2], [15]. A growing number of meteorological studies is addressing the Arctic climate system. But, overall, coverage is still limited. This, in turn, limits the knowledge achieved in the studies.

Better understanding and observation of the polar regions will act positively not only for these regions themselves, which would benefit greatly from improved weather forecast or natural hazard assessment, but also for lower latitudes. Global weather forecasting is dependant on observations from the polar regions [14]. Also, the polar regions interact with lower latitudes through an abundance of different phenomena, which are essential e. g. for mid-latitude climate change.

This is because Arctic amplification, the increased sensitivity of the Arctic weather and climate system to global warming, influences climate change in the mid-latitudes through teleconnections. Increasing of the geopotential thickness over the Arctic, weakening of the thermal wind, stratospheric pathways for heat fluxes and ensuing changes to the global circulation patterns have been linked to weather extremes and lessened warming in observations of mid-latitude winter [3] and to persistent dry-spells and heat in summer [4].

Precipitation is a key variable in Arctic amplification and the effected teleconnections. As part of the hydrological cycle, precipitation patterns preside over the mass balance of glaciers and consequentially the rise of sea levels, or the freshwater inflow of oceans and the global ocean circulations [9]. It also substantially effects the radiation feedback of land and ice surfaces, as the surface albedo changes with soil humidity, or the characteristics of snow cover. Yet there are a number of challenges attached to precipitation observation and monitoring, as expounded upon in chapter 1.4.

1.3 SVALBARD

1.3.1 *Research Site Svalbard*

Within the Arctic, the archipelago of Svalbard is a unique vantage point for studying weather and climate. The town of Longyearbyen offers a very good scientific infrastructure, unrivalled at such high latitudes. Also, Svalbard lies

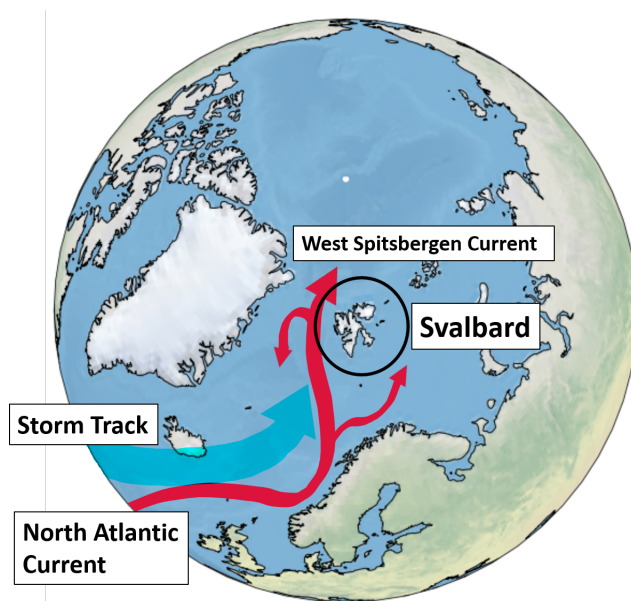


Figure 1: Map of Svalbard region, including schematic illustrations of the West Spitsbergen Current and Atlantic storm track.

squarely in the middle of the meteorological and oceanographic gateway to the central Arctic. The West Spitsbergen Current brings oceanic heat from more southern parts of the Atlantic ocean into the Arctic past Svalbard's coasts [28]. Atmospheric heat is transported into the central Arctic primarily via cyclone activity following the Atlantic storm track [29]. These cyclones are also associated to the gross of precipitation that falls on Svalbard [29].

1.3.2 Precipitation on Svalbard

Svalbard, and especially Longyearbyen, has a relatively dry climate. It is part of the Arctic desert, with only few months in the year in which liquid water is routinely present. There are ca. 700 mm of precipitation on Svalbard per year [27]. Mostly it falls in the mountainous regions in the west. Sheltered valleys at low elevations are driest. Longyearbyen, located in a rain shadow area on the coast, gets less than 200 mm of precipitation per year [27]. Generally precipitation intensities are low. But extreme events with high precipitation intensities are not unheard of [6].

1.3.3 Precipitation on Svalbard in a Changing Climate

Climate change is expected to have - and has already had - a large effect on precipitation in the Arctic ([21], [19]). This can also be seen regionally in places including Svalbard ([12], [8]), the Atlantic sector in general [17] and the Eurasian continent ([18], [30]). The Arctic is warming multiple times faster than the global average [20], due to Arctic amplification. In fact the weather station at Longyearbyens airport has recorded a warming by 7.8°C from 1971 to 2017, which is more than nine times the global rate of 0.83°C in the same time period [12]. The warmer air is able to hold more moisture. This does not have a direct effect

on the intensity of precipitation, as precipitation is a rate of change of humidity, rather than that humidity itself. But, it does increase the maximal possible intensity for each precipitation event. In Eurasia, a shift of precipitation patterns towards fewer low intensity and more high intensity events could be observed, especially outside of summer, when the availability of moisture is a limiting factor [30]. This indicates a realization of the higher intensity potential, given by rising temperatures, for this region. The rising temperatures simultaneously make more of that precipitation fall as rain instead of as snow, as shown for the European sector in Łupikasza and Cielecka-Nowak, 2020 [17]. Here, changing global oscillation patterns additionally lead to an increase in extreme precipitation such as rain on snow events, which are associated with strong southwesterly flows, bringing large amounts of warm moist air into the high Arctic even in winter ([6], [29]). For Svalbard in particular the coming decades are predicted to bring an increase of precipitation with a higher maximum of annual snow storage, but also a decrease in the percentage of solid precipitation and snow cover duration [12]. Viewed from the perspective of natural hazard assessment this means increasing risks for Svalbard's communities.

1.4 OBSERVATIONAL CHALLENGES

There are multiple challenges to an analysis of precipitation patterns in the Arctic. And these challenges are of a main interest to this study.

Foremost, representative sets of sufficiently long observation time series are hard to come by, as mentioned in 1.2 and experienced during the study.

Also, the patterns and phenomena in question exhibit a great spatial and temporal variability [14], making their detection vulnerable to the choice of frame. Depending on what spatial and temporal limits are chosen for the included observations, the deduced patterns will change, making it difficult to forge them into a big picture. Precipitation is more variable than temperature [1]. And Svalbard and the Atlantic sector convey additional variability through their complex topography and the air-ice-sea interactions, which cause great climate variability on inter-annual to inter-decadal time scales.

Measurement of precipitation in Svalbard is also in itself a difficult feat. Precipitation in Svalbard is often accompanied by strong winds [29]. This leads to an exacerbation of the *undercatch* problem (see more on this in chapter 4.2.1). Undercatch is a systematic measuring error afflicting precipitation gauges, mostly caused by aerodynamic blockage of the gauge opening in windy conditions, but also by wetting and evaporational losses [10]. Solid precipitation is effected a lot more by undercatch than liquid precipitation [10]. On Svalbard, the combination

of windy conditions and predominantly solid precipitation emphasizes the need for adequate correction models [9].

An additional problem for measurements is caused by blowing snow. The strong winds in Svalbard lead to large mass movements of snow, critically influencing the snow distribution. Also, snow is blown into or out of precipitation gauges, or past distrometers, distorting the measurements with additional systematic error.

Quite apart from the systematic offsets in measurements due to undercatch, blowing snow or local topography, fieldwork in the Arctic comes with its own set of obstacles. This thesis came with a large practical portion. And, thus, I have learned to use wrenches and screwdrivers with mittens on my hands and to keep zip ties close to my body so they don't break in the cold. Finding batteries that can cope with the cold can take several failed attempts. Measuring snow depths manually, with an avalanche probe, was also more difficult than first anticipated. There are often ice layers within the snow cover. And it was nearly impossible to know whether the surface I hit was the actual ground or ice until I broke through. This problem was exacerbated by the broken rock terrain on which I worked. Finally, also the local inhabitants of my measuring sites would occasionally cause problems. Several days of missing data from one of the sites are the work of an arctic fox chewing through my cables.

1.5 RESEARCH QUESTIONS

This thesis delves into the exploration of snow depths in the Longyearbyen area by experimental meteorological means. The means of this study included snow depth measurements and standard meteorological measurements of temperature, wind and precipitation at several points around Longyearbyen. They also included state of the art weather model and snow model data. They did not include observations of snow pack layerings or densities. Hence, the meteorological perspective hereby means concentrating on the influence of meteorological parameters, such as precipitation and wind, on only the depth of the snow cover. The depth of the snow cover, of course, is not independent from its density, which must therefor somehow be accounted for. This is done by using constant parameters from literature or by including the snow model. It imbibes those variables native to snow studies such as layering, aging and density, otherwise overlooked by the meteorological perspective.

Within this setting, the following question is asked. What controls the snow depth? As this thesis has a large practical, experimental portion, the question

falls into two separate research questions.

1. On a practical note: Can the (point) observations made here represent the spatial and temporal distribution of snow depth in the area? Does the snow model reproduce the observed snow depths faithfully? And can those recorded or modelled snow depths be used as a benchmark for further analysis of dependencies, e. g. to correct for the observational bias in precipitation gauges?
2. On the analysis of dependencies of the snow depth from certain meteorological processes: Are there meteorological parameters that serve well as proxies for variations in the snow depth? In this thesis precipitation and wind were examined.

The study is based on the spring snow season of 2022. Additionally, longer time series of some meteorological parameters from permanent weather stations are considered.

1.6 OUTLINE

A number of simple distance based snow depth sensors were deployed on the slopes around Longyearbyen². In addition snow depths are similarly measured by the weather stations in the area run by Met Norway³. Chapter 2 discusses these snow depth observations. It focuses on the first research question, investigating the ability of these point measurements to depict the snow depth patterns of the entire area and time frame. This chapter raises the issue of strong local variability, which is elucidated in a case study.

Chapter 3 looks at the snow depths modeled by the SeNorge model⁴ and compares them to the observed snow depths. This contributes to the first research question, asking whether the model, which imbibes precipitation, melting, sublimation and compression of the snow layer, but not transport with wind, is capable of representing the snow depth patterns in the area. But it also taps into the second research question. A good representation would confirm the choice the model makes with the meteorological parameters it uses, in particular the insignificance of wind transport.

The next two chapters match the evolution of the observed snow depths with probable contributing parameters, with a chapter of the thesis dedicated to each

²<https://www.unis.no/arctic-safety-centre/driva>

³<https://seklima.met.no>

⁴<https://www.senorge.no/Snowmap>

precipitation and wind. This addresses the second research question, evaluating each parameter as possible proxy for snow depth variations.

In chapter 4 this is done for precipitation. It was taken care to correct the precipitation for the known undercatch problem. And it was assessed in what way the snow depth measurements can help with this.

Wind, as a controlling factor in the snow depths evolution, is investigated in chapter 5. Both wind speed and wind direction are looked into as possible proxies for changes in snow depth.

Finally, chapter 6 contains a summarizing discussion of the results achieved with respect to the research questions and conclusion of and outlook onto the contribution of practical meteorological methods to monitoring and analyzing the local evolution and distribution of snow in the Longyearbyen area.

SNOW DEPTH OBSERVATIONS

This chapter introduces the heart piece data set of the thesis - the snow depths measured around Longyearbyen, which are used in all the chapters to come. This data set is explained and processed. Its limits regarding the representation of snow depth distributions are pointed out.

2.1 SETUP AND INSTRUMENTATION

2.1.1 *Setup*

There exists a network of snow depth sensors around Longyearbyen, operating on simple distance measuring techniques. The sensor is mounted approximately 2m above ground, pointing downwards and measuring the distance to the surface, which will decrease with rising snow levels.

Such sensors belong to the standard fitting of Met Norway's weather stations (operating according to the standards set by the World Meteorological Organization) of which there are three operational in Longyearbyen's direct vicinity¹. These are located in relatively flat terrain and are spread across the larger Longyearbyen area.

In 2019, UNIS, Telenor and Longyearbyen Lokalstyre joined together in the DRIVA-project². Six snow depth sensors were set up around Longyearbyen, to be used in local avalanche forecasting. They are hereafter referred to as the DRIVA sensors. They monitor the snow accumulation in avalanche prone slopes directly overlooking the town, providing a more detailed view of the valley.

For this thesis an additional weather station, the *super site*, equipped with two different snow depth sensors as well as temperature, humidity and wind sensors on one height, was put up on a slope thought to be safe concerning avalanches, due to an avalanche fence in direct proximity. During the course of the study

¹<https://seklima.met.no>

²<https://www.unis.no/arctic-safety-centre/driva>

Table 1: The super site was equipped with the instruments listed in the table. The table shows measuring gaps (only considered when lasting at least 24 hours). Note: The Aurora has less measuring gaps than the SNOdar because the SNOdar had battery issues.

Instrument	Measuring Gaps
Thermo- /Hygrometer and Anemometer	... - 05.03.2022
	13.03.2022 - 22.03.2022
	09.04.2022 - 10.04.2022
	26.04.2022 - 13.05.2022
	25.05.2022 - 27.05.2022
	02.06.2022 - ...
Aurora	... - 14.02.2022
	23.05.2022 - 24.05.2022
	31.05.2022 - ...
SNOdar	... - 11.02.2022
	04.03.2022 - 10.03.2022
	16.03.2022 - 29.03.2022
	29.05.2022 - ...

period, the super site had to be moved once, due to the building of a ski lift across its original location. It was shifted up the slope slightly, but stayed next to the same avalanche fence. The super site and its instruments (in the second location) are seen in figure 5. Table 1 shows the measuring gaps of the instruments which were caused by battery failures and fox bitten cables.

A list of the observation sites used can be found in table 2. A map of their locations can be found in figure 2. The super site's first location is referred to as *Super Site I*, the second location as *Super Site II*.

In chapter 5 additional data from a weather station on the plateau of Gruvefjellet will be used. This station does not boast a snow depth measuring device and is not discussed before chapter 5.

2.1.2 Instrumentation

The snow depth sensors used here work on slightly different measuring principles. The Met Norway stations use *Lufft SHM31* lidar (light detection and ranging)

Table 2: List of all snow depth observation sites. The sites were operated by Longyearbyen Lokalstyre (Huset High/Low, Nybyen North/South and Sukkertoppen High/Low), UNIS (Super Site) and Met Norway (Adventdalen, Airport and Platåberget).

Name	Location	Elevation	Slope	Instrument	Logging Interval
Huset High	78.2084N, 15.5695E	310m	38.44°	DRIVA (sonar)	11min
Huset Low	78.2072N, 15.5819E	121m	23.7°	DRIVA (sonar)	11min
Nybyen North	78.2043N, 15.6257E	368m	37.63°	DRIVA (sonar)	11min
Nybyen South	78.2002N, 15.6012E	216m	28.25°	DRIVA (sonar)	11min
Sukkertoppen High	78.2118N, 15.6539E	325m	34.02°	DRIVA (sonar)	11min
Sukkertoppen Low	78.2144N, 15.6516E	166m	26.64°	DRIVA (sonar)	11min
Super Site I	78.2156N, 15.6595E	124m	15.58°	Aurora (sonar), SNOdar (radar)	31min
Super Site II	78.2149N, 15.6581E	148m	16.64°	Aurora (sonar), SNOdar (radar)	31min
Adventdalen	78.2022N, 15.831E	15m	0°	lidar	1min
Airport	78.2453N, 15.5015E	28m	0°	lidar	1min
Platåberget	78.2278N, 15.378E	450m	0°	lidar	1min



Figure 2: Winter satellite image of the Longyearbyen area from <https://toposvalbard.npolar.no/>, with locations of snow depth observation sites. North orientation straight upwards.

sensors. The super site hosts a *SensorLogic SNOdar*, which uses radar (radio detection and ranging), and a *Vicotee Aurora*, which uses sonar (sound navigation and ranging). The DRIVAs use the same type of sensor as the Aurora (*HRXL-MaxSonar-WRS*), but are mounted in cheaper printed housings. Note: Sensors put up in slopes expected to have a high avalanche risk are naturally expected to be caught in avalanches every now and again. Such sensors should be low-cost.

They all send out pulsed signals (ultra-sonic sound waves in the case of the DRIVAs and the Aurora, microwave radiation in the case of the SNOdar and visible short-wave radiation in case of the SHM₃₁ lidars). The travel time of the signal reflected from the snow surface is then used to compute the distance.

Distance measurements of relatively smooth surfaces at distances as present here (< 5 m) are fairly accurate for all three measuring principles used. The data is given with a resolution of 1 mm for each instrument used here. Shorter wavelengths (in lidars) can theoretically resolve the surface structure with higher accuracy. Yet, this is not necessarily a desired property for monitoring snow depths over longer periods of time. Lidars also boast a greater maximal range, though this is not relevant for the distances measured here. Lidar distance measurement's dependency on color is not a problem with the homogeneously white snow surface, though transparency may cause problems. Radars and sonars,

on the other hand, have the advantage of penetrating disturbances such as fog or blowing snow better, due to their longer wavelength, though they may also penetrate the snow cover, depending on the refractive index. Sonars are the most cost-efficient choice.

Sonars, because of their use of sound waves, are temperature dependent in their distance measurements. The speed of sound is

$$c = \sqrt{\frac{c_p}{c_v} R_0 T_v}, \quad (1)$$

with the heat capacity ratio of dry air $\frac{c_p}{c_v} = 1.4$, the specific gas constant for dry air $R_0 = 287.1$ and the virtual temperature T_v . The speed of sound varies with temperature on scales relevant to the distance measurements, while the variation of the speed of light in cold or hot air masses does not effect the distance measurement significantly. Outside of polar night, this results in a daily cycle in sonar observations. Post-processing must be applied to correct for this.

2.2 POST-PROCESSING

The snow depth measurements from Met Norway are already post-processed. They present smooth, gradual time series. This is not the case for the Longyeardalen sensors however (DRIVA sensors and the sensors on the super site). They were first corrected for temperature and slope, then subjected to a sanity mask and finally resampled to 1 hour logging intervals before being used in the analysis. In figure 4 the effects of correction and post-processing on the Longyeardalen sensors can be seen.

2.2.1 Temperature Correction

The HRXL-MaxSonar-WRS sensors (in the DRIVA sensors and the Aurora on the super site) automatically correct for temperature, using the internal temperature of the instrument. Ironically though, this introduces the exact same diurnal cycle it is supposed to correct for, while without this automatic correction there is none. It may be that while the housing or mounting of the sensor heats up whenever they are in the sun, the same is not true for the air between snow cover and sensor. In this case the instrument would correct for the higher temperature of its case instead of the unchanged air temperature determining the speed of the sound signal. A better correction is thus achieved when applying the correction's inverse to the data, hence reversing the correction falsely applied by the instrument. After that, a more genuine temperature correction could be applied, based on air temperatures measured outside the instrument casing. However, this is not

an option for the DRIVA sensors, as no external thermometer is installed with them.

Hence, the temperature correction is done as follows. Let d be the original, uncorrected distance reading and d_{corr} be the falsely corrected distance, in metres. Let t be the time of flight in seconds and T be the temperature in ° Celsius. The automatic temperature correction used by the HRXL-MaxSonar-WRS is

$$d_{corr} = \frac{t}{2} \left(20.05 \sqrt{T + 273.15} \right). \quad (2)$$

When approximating the virtual temperature with the absolute temperature, the speed of sound is

$$c = 20.05 \sqrt{T + 273.15}. \quad (3)$$

The instrument is calibrated at 0°C. Thus

$$d = \frac{t}{2} \left(20.05 \sqrt{273.15} \right). \quad (4)$$

This results in the temperature correction

$$d_{corr} = d \sqrt{\frac{T + 273.15}{273.15}}. \quad (5)$$

The reverse correction is therefor

$$d = d_{corr} \sqrt{\frac{273.15}{T + 273.15}}. \quad (6)$$

From here a correction with the air temperature from outside the instrument housing can be commenced. For T_A the air temperature in ° Celsius, the true corrected distance is then

$$d_{true} = d \sqrt{\frac{T_A + 273.15}{273.15}}. \quad (7)$$

As the air temperatures are not available for the DRIVA sensors, the distances used in the remainder of this study are d , instead of d_{true} .

2.2.2 Slope Correction

While the temperature correction is only critical for the sonar sensors, all data has to be corrected for inclination of slope. A slope in the footprint of the sensor

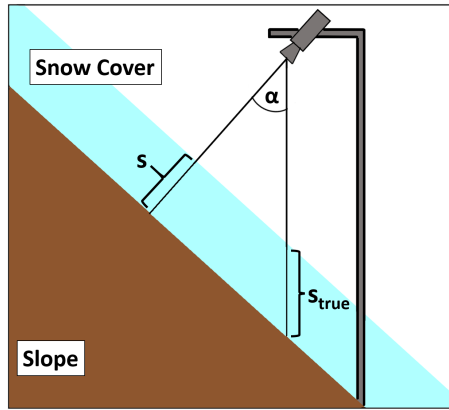


Figure 3: Schematic for slope correction.

introduces uncertainty, which can be avoided by pointing the sensor orthogonally to the slope and correcting for the ensuing error (schematically explained in figure 3) in the post-processing. This was done for the sensors used in this study. The correction in post-processing is simple. Let α be the inclination of the slope and s be the measured snow depth. Then the true snow depth is

$$s_{true} = \frac{s}{\cos \alpha}. \quad (8)$$

This correction results in a constant offset of the snow depth time series.

2.2.3 Unphysical Values

The data set is now corrected for temperature and slope. But it still contains a lot of noise. In order to reduce this, several sanity masks were applied to weed out unphysical values. Their conditions for rejecting a value are displayed in table 3. The effect of this sanity mask can be seen in figure 4, where part (a) shows the time series prior to applying the sanity mask.

2.2.4 Resampling

For comparability the snow depth measurements of the different instrument sets were all resampled to 1h intervals after being corrected and run through the sanity masks.

Table 3: The table shows the mask for rejecting unphysical values in the snow depth data from DRIVA sensors and super site. x is the corrected value for the snow depth in mm.

Condition	Explanation
$x < 0$	Negative snow depths
$x > 1800$	Snow depths higher than 1.8m
$ x_t - x_{t-1} > 100$ for x from DRIVA	sudden jumps in snow depth of ca. 10cm/10min
$ x_t - x_{t-1} > 300$ for x from super site	sudden jumps in snow depth of ca. 30cm/30min

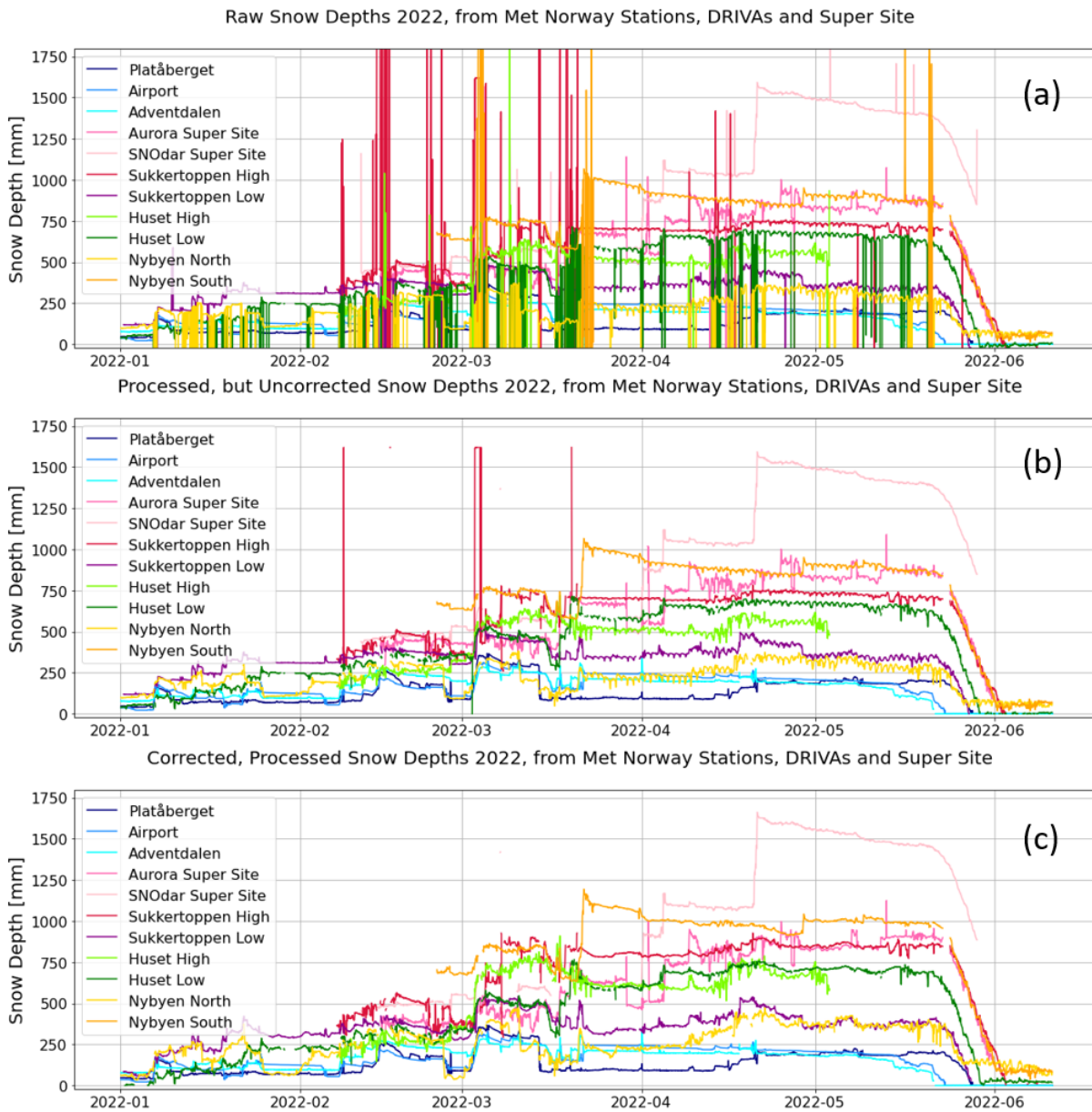


Figure 4: Observations of snow depths from Longyeardalen sensors (DRIVAs and super site) and Met Norway stations, resampled to 1 hour logging interval. Several processing steps are shown. The Met Norway data was pre-processed, so processing in this figure refers to processing of the Longyeardalen sensor data. (a) Uncorrected and unprocessed snow depth measurements. (b) Snow depths after applying sanity mask, but without correcting for diurnal cycle or slope. Note: The outliers in the Sukkertoppen High time series are eliminated when first correcting for temperature and slope, as their corrected values are greater 1800. (c) Snow depths after applying sanity mask and correcting for diurnal cycle and slope.

2.3 RESULTS

2.3.1 *Processed Data Set*

The processing of the data yielded results in their own right. Because of this the data set was recorded and preserved in each processing step. The resulting file was handed in along with the thesis and will hopefully soon be accessible via the Pangaea Data Publisher.

Each processing step corresponds to a separate level data set. In the file, the variables of the original data set (level-0) are signified by a „_0“. The level-1 data set is derived from the original, level-0 data set by correcting for slope and temperature. Its variables are signified by a „_1“. The level-2 data set is derived from the level-1 data set by applying the sanity mask from table 3 and resampling to 1 hour logging interval. This is the final data set used for the rest of the study. Its variables are signified by a „_2“. The time series shown in figure 4(b) was only created to illustrate the temperature correction. It was derived from the level-0 data by applying the processing mask from table 3. The corresponding variables are signified by a „_1A“.

2.3.2 *False Temperature Correction*

It was found that the automatic temperature correction in the DRIVA sensors introduces an error in form of an artificial diurnal cycle outside of polar night (see figure 4(b)). This is thought to be a result of the temperatures necessary for correction being measured inside the housing of the instrument, which heats up more than the air between sensor and snow cover when in the sun. As the actual air temperature is not measured and an additional instrument would be needed to do so, increasing instrument costs, a simple reversal of the automatic temperature correction is advised. This yields a realistic snow depth time series (see figure 4(c)).

2.3.3 *Locality of Spatial Distribution as seen at Super Site*

The super site was originally put up as a calibration station, to provide calibration data for evaluating the performance of the DRIVA sensors. Its two snow depth sensors (the Aurora, of the same sensor type as the DRIVAs, and the SNOdar, using a different measuring principle) were meant to be compared to each other and matched to regular manual readings. The manual readings were conducted approximately weekly and consisted of measuring directly beneath the sensors with an avalanche probe, measuring a couple of meters away with a

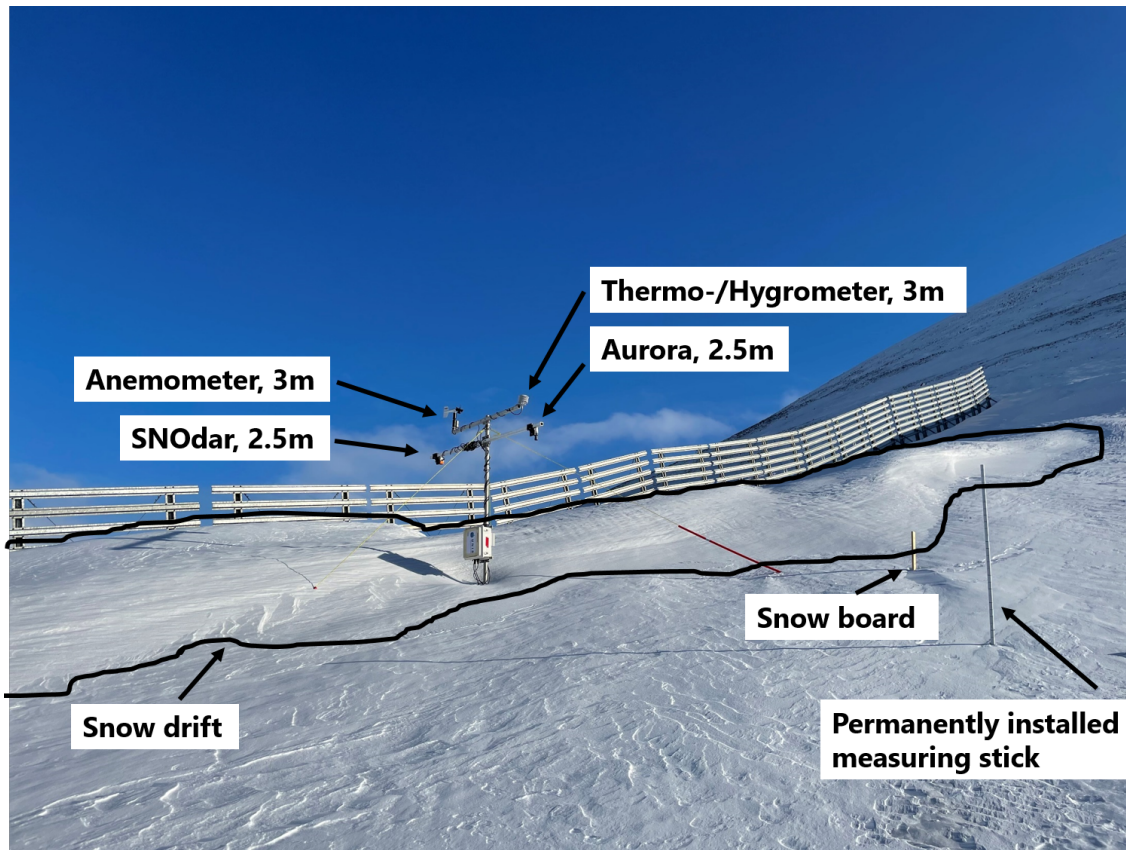


Figure 5: Setup of the super site with mast, measuring stick and snowboard. The snow drift can be seen creeping in from the direction of the fence.

permanently installed measuring stick and of measuring snow accumulated since the last reading with the help of a mobile snow board. The setup can be seen in figure 5. The location of the super site was chosen to be on a slope comparable to the slopes the DRIVA sensors occupy, but without the immediate avalanche risk, so as to enable regular visits. Thus, it was decided to place the super site next to an avalanche fence on Sukkertoppen mountain.

The close proximity of the snow depth sensors was thought to ensure their measuring of the same physical properties. This however turned out to be false, as the avalanche fence caused a snow drift to form in its lee. The snow drift crept beneath the SNOdar-sensor, but never reached the Aurora. It caused a rather dramatic jump in the SNOdar's snow depth time series, when within only a few hours the snow level underneath it rose by almost 60cm (see figure 4 on 20.04.2022). Even the 2m of boom separating the SNOdar- and Aurora-sensors sufficed to let them measure vastly different snow depth realities.

This has consequences for the general feasibility of estimating snow distributions with point measurements such as these. The high degree of independence between observations done in close proximity makes a meaningful interpolation of the observations impossible without further input on the dependencies of the snow depth.

2.3.4 *Representativeness of Observations of Snow Depths in Longyearbyen Area*

The locations of the snow depth sensors were not chosen representative of the area as a whole. They were chosen to monitor slopes around Longyearbyen with a high avalanche risk. These slopes are expected to have higher snow depths than most other parts of the area. Therefore, estimates of the total amount of snow in the area can not be made by simple averages of these observations.

2.3.5 *Elements Evident in Temporal Evolution*

While spatial representation of snow depth distributions has been seen to be poor, the temporal variations picked up by the observations exhibit a satisfying degree of collective behaviour. Several types of features can generally be observed (as in figure 6).

There are times at which snow depths at all sites increase simultaneously (e. g. figure 6, I). When compared to meteorological parameters from the Met Norway stations (figure 6 (a) and (c)), these times appear to coincide with calm winds and precipitation at below freezing.

Periods of time with elevated wind speeds tend to be more chaotic in the variation of snow depths. This is especially apparent in mid March (e. g. figure 6, II), when a polar low determined the weather over Svalbard. Temperatures rose above freezing in a winter warm spell and great amounts of rain fell in a rain on snow event. This was accompanied by very strong winds. The resulting variations in the snow depths are immensely chaotic.

There are also times with simultaneous decrease in snow depth at all sites (e. g. figure 6, III). These times coincide with calm winds, temperatures below freezing and a general lack of precipitation. It seems the snow cover is settling in these times, maybe growing more compact or else sublimating.

Finally, at the end of the season, melting sets in for all the sites at approximately the same time and at approximately the same rate. A temperature probe in

the snow at the super site sets the beginning of the melting (when the snow temperature rose to 0°C) to midday on 21.05.2022.

2.4 DISCUSSION AND SUMMARY

How do these results relate to the first research question: Do the observed snow depths represent the depth of the snow cover in the Longyearbyen area in its spatial and temporal variation?

2.4.1 *Spatial Distribution of Snow Depths in Longyeardalen*

The spatial distribution of snow depths around Longyearbyen is impossible to be deduced from the snow depth observations alone. The foremost reason for this is the very high spatial variability on very small scales (see chapter 2.3.3).

But also, the unrepresentative choice of locations for snow depth measurements (made to monitor imminent avalanche risk, not general snow distributions) makes the DRIVA sensors a less than ideal tool to gain an overview over the spatial distribution of snow in the Longyearbyen area.

There is a chance at estimating the distribution indirectly, though. If the following chapters succeed in finding good proxies for the variation of snow depths, these can be taken as leads to guess at the snow depth of a certain place based on the local conditions of said proxy.

2.4.2 *Temporal Evolution of Snow Depths in Longyeardalen*

The temporal variation of the snow depth in the Longyearbyen area is represented better than the spatial one in the snow depth measurements. Common features can be seen in the time lines for the snow depths from the different sensors (see figure 6). This points to their ability to represent such changes as imbued by large scale events like heavy precipitation or lack thereof. These effects seem to be superimposed with more local changes. Hints as to the effects of more local conditions, such as wind, may thus be found in the relative difference of the snow depth time lines.

2.4.3 *Summary*

The automatic temperature correction done by the sonar sensors, using internal cabinet temperature, was found to be counterproductive. Ideally a temperature correction using the air temperature between sensor and snow cover should be

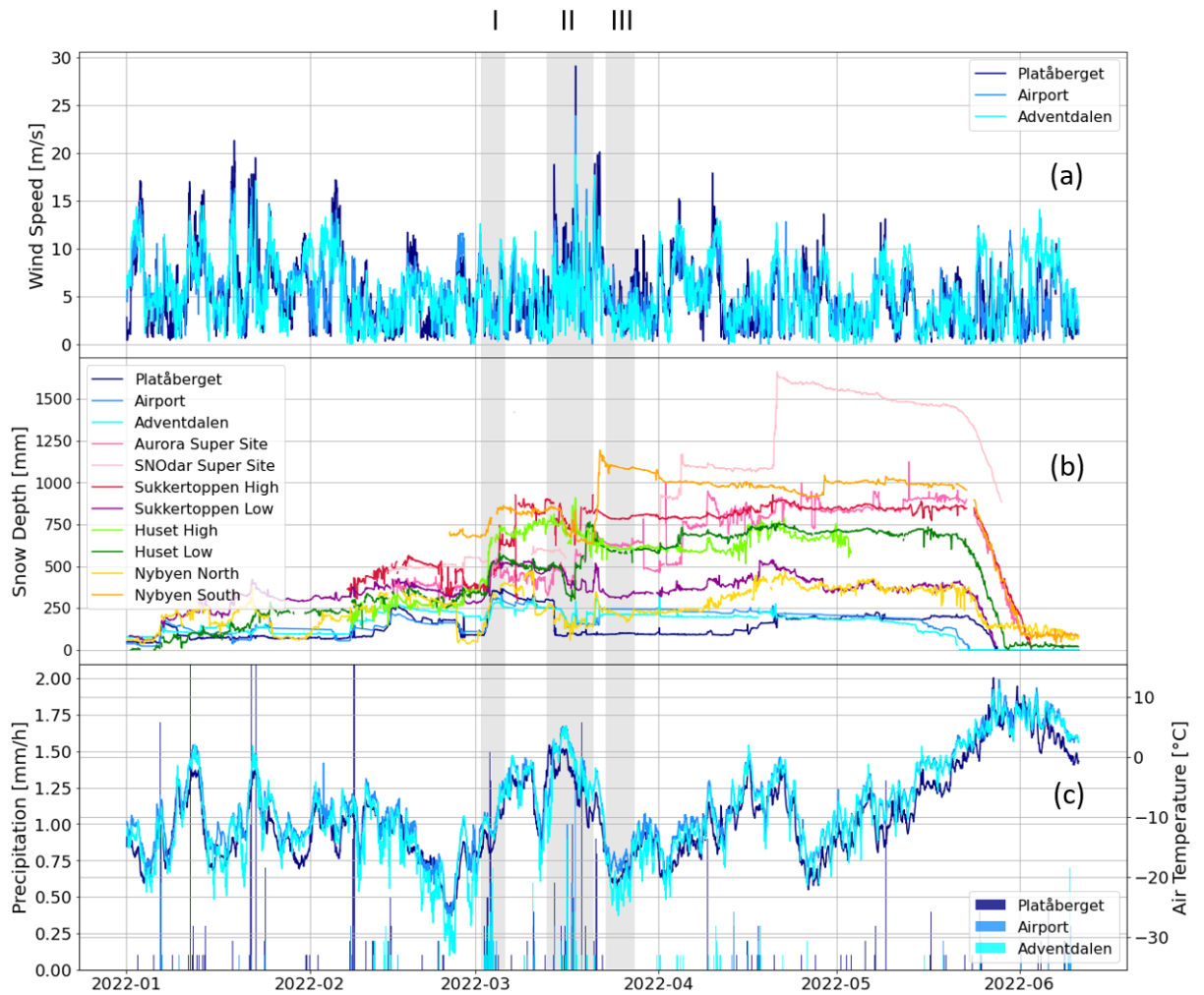


Figure 6: Some general features of the snow depth observation time lines can be linked to meteorological events seen in Met Norway's weather station data. This includes: I) strong precipitation in relative calm, seen as general increase in snow depths; II) strong precipitation with strong wind and intermittently positive temperatures, seen as chaotic time period in snow depths; III) no precipitation and relative calm, seen as synchronous slight decrease in snow depths.

used. Lacking this measurement, it should at least be abstained from correcting with the internal cabinet temperature.

Concerning the first research question (Do the observations represent the snow depth in its spatial and temporal variation?), a divided answer should be given. It may not be possible to gauge absolute estimates of the spatial distribution of snow depths or even just the mean amount of snow in the area from the snow depth observations alone. But the temporal evolution of the observation time series represents larger scale changes in its common features, as well as individual variations when looking at the time series's differences.

MODELLED SNOW DEPTHS

Spatially varied research objects, such as snow depth distributions in the Longyearbyen area, profit greatly from the model point of view. The model allows for a comprehensive perspective onto spatial variations of an area, not granted by scant or scattered point measurements. Of course, to adequately represent reality, a model must contain the relevant processes and represent or parameterize them on the relevant scales.

3.1 DESCRIPTION OF THE MODEL

For this study the SeNorge snow model¹ provided modelled snow depths on a 1km x 1km grid scale for a 3h time step, depending largely on temperature and precipitation data. The version of the model used is a new, not yet operational, branch specifically looking at Svalbard. SeNorge's snow model prominently lacks the effects of wind transport. This, however, offers a chance of isolating temperature and precipitation effects from wind effects on snow cover depth.

In the model the accumulation of snow in a grid cell, as schematically visualised in Figure 7, is caused by the combination of precipitation and surface air temperatures $<0.5^{\circ}$ C. The surface air temperatures will also effect the density of the accumulated snow. The snow pack has the capacity to store liquid water. Liquid water from rain or from melting will compactify the snow pack until the liquid water content threshold is reached. After that the liquid water will disperse as runoff. Apart from by accumulation, the snow pack evolves by melting and by compaction. Each is controlled by different parameters depending on, in compaction's case, prominently wind and time and, in melting's case, temperature and incoming solar radiation.

The snow depths simulated by the SeNorge model are a good estimate of changes triggered by larger scale processes such as precipitation or temperature

¹<https://www.senorge.no/Snowmap>

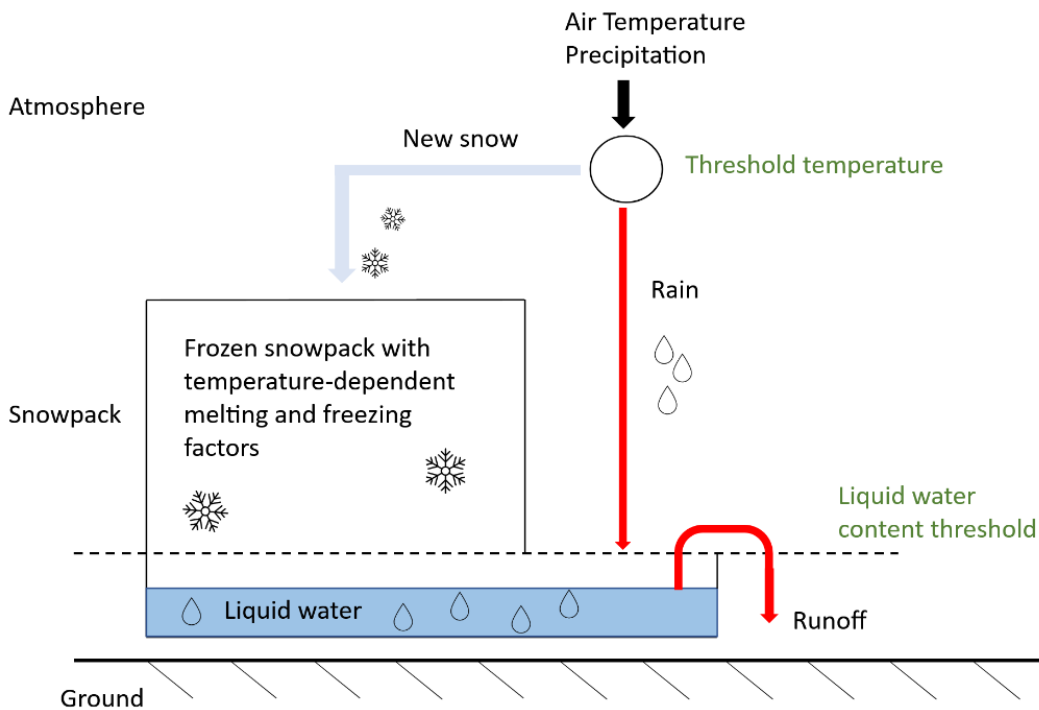


Figure 7: Simplified schematic of processes included in SeNorge snow model. From <https://www.senorge.no/Snowmap>.

fields. Errors in this representation arise either from inaccuracies in the tuning of the model or from sub-scale processes missed by the input fields of temperature and precipitation, which are taken from the local operational weather forecast model, AROME Arctic². It has a 2.5 km grid scale and it does not assimilate precipitation observations. There hence might be short-lived or local variations in temperature and precipitation which are not included in the model input. Similarly, the model output cannot be expected to distinguish sub-scale variations.

3.2 RESULTS

3.2.1 Results from Modelled Data

Within the spring snow season of 2022 (01.01.2022 - 10.06.2022) the mean modelled snow depths of the area around Longyearbyen range from only a couple of millimetres at the coast to 50 cm higher up in the valley heads (see figure 11). Their temporal evolution can be seen in figures 13 and 15. For the entirety of Svalbard the season mean of modelled snow depths can reach more than four metres (see figure 8).

²<https://www.met.no/en/projects/The-weather-model-AROME-Arctic>

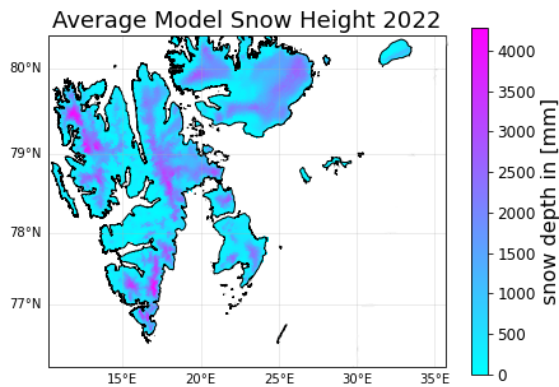


Figure 8: Mean season snow depth from SeNorge.

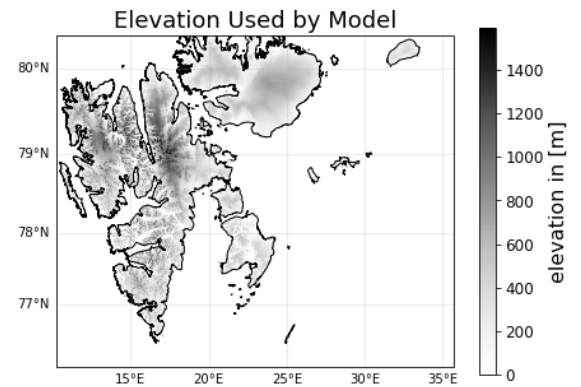


Figure 9: Elevations used in SeNorge model.

When comparing the figures 9, which shows the elevations used by the model, and 8, showing the season mean snow depth, one is struck by a certain similarity. This similarity can be quantified further by taking a look at the correlation between elevation and mean seasonal snow depth. A statistical analysis of this property is beyond the scope of this study. But a visualization of the season mean snow depth and the elevation of the grid boxes in a 2D-histogram (see figure 10) shows two main branches, both testimony for increasing mean snow depths with increasing elevation.

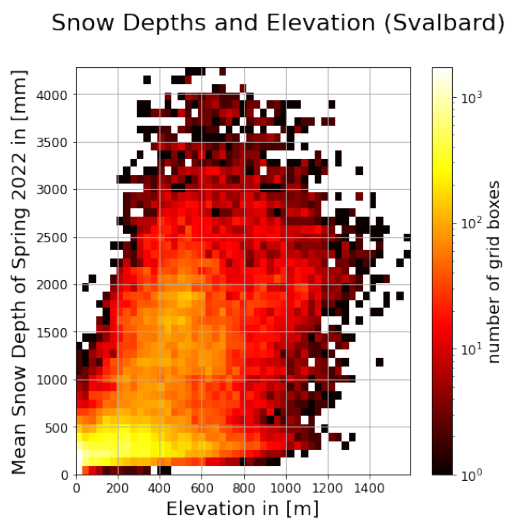


Figure 10: Histogram of mean season snow depth and elevation per model bin. Two branches are visible, with increasing snow depth for increasing elevation.

Elevation dependency of precipitation is often found in mountainous settings, where orographic precipitation is typical. But, for Svalbard, such orographic precipitation patterns are superimposed with the maritime precipitation patterns induced by its island position. These feature larger amounts of precipitation for the western side of the archipelago. Most precipitation is brought to Svalbard from the west with cyclones picking up moisture over open, warmer Atlantic waters [29]. To the east of Svalbard it is drier. This is also due to the sea ice, which is abundant there in the spring snow season. The pattern of season mean snow depths seen in figure 8 is thus the result of two main influences: elevation and archipelago aspect.

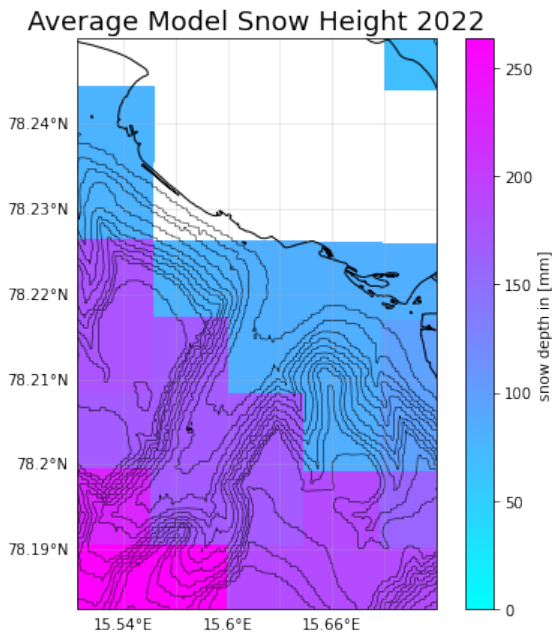


Figure 11: SeNorge snow depths shown on a map of Longyeardalen. These are the average snow depths for the first 6 months of 2022.

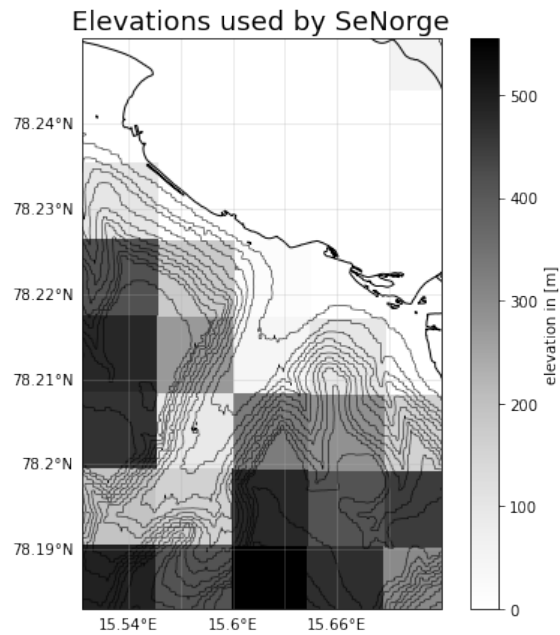


Figure 12: Elevations used by SeNorge shown on a map of Longyeardalen.

In figure 11, the season mean snow depth exhibits a general increase with increasing distance from the fjord. Though this is a reasonable hypothesis, as the open water of the fjord is a sink for wind transported snow, the model, which does not include wind transport, is unlikely to pick up on it.

3.2.2 Comparison with Observations in the Spatial Dimension

Comparing the modelled snow depths from SeNorge to the measured snow depths of the snow depth sensors around Longyearbyen requires caution. A careful consideration of the scales and processes involved is crucial.

Spatial resolution is sure to have a marked effect on the feasibility of comparing the model to the individual observation sites. A quick look at figure 12 explicates the issue. SeNorge's resolution is (barely) sufficient to resolve the Longyear valley. But the snow depth sensors on the valley slopes occupy only three different grid boxes of the model. A statistical comparison is not possible with such a scant sample.

The following paragraphs take the observations from the snow depth sensors around Longyeardalen as a benchmark. They are compared to the model's time

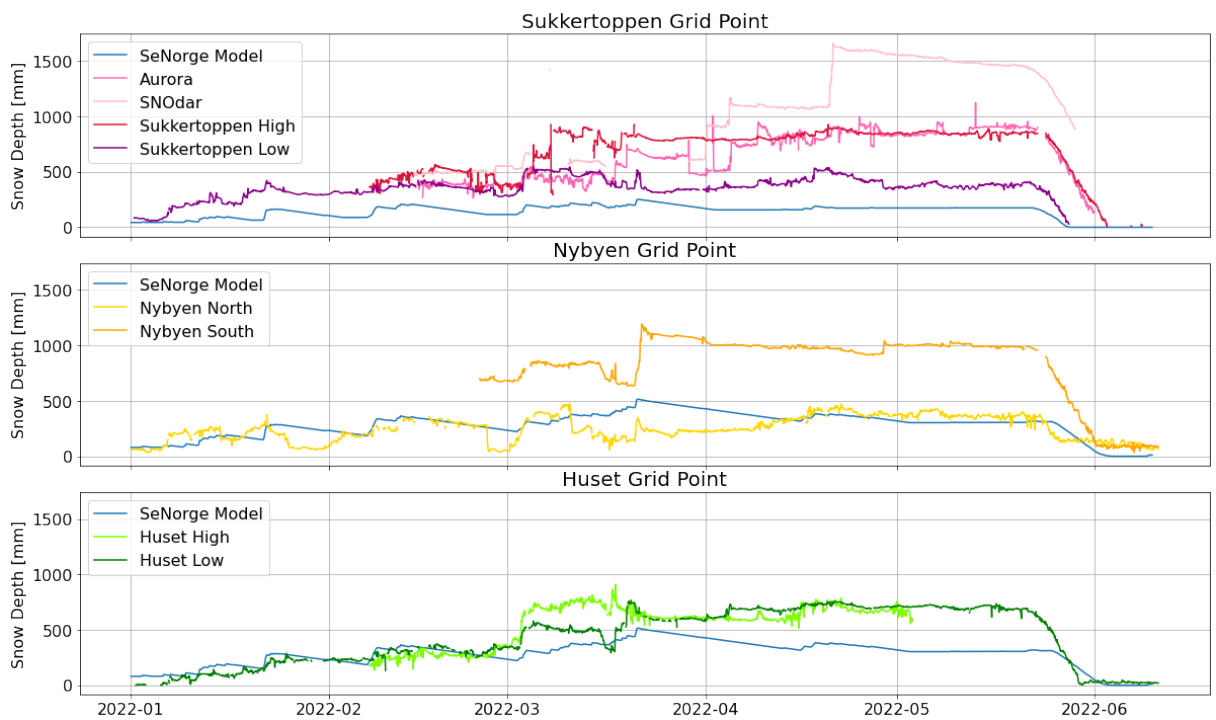


Figure 13: Observed snow depths compared to SeNorge snow depths of nearest grid point.

series, first attempting a case study verification of spatial distributions for the three grid cells covered by observations (in the following two paragraphs) and then, in 3.2.3, of temporal evolution as predicted by the model.

Nearest Grid Point Approach

When simply taking the model to be the best representation of snow depths in each grid box and choosing to compare each observation site to its nearest grid point, the Longyeardalen sensors divide into three different grid boxes, as shown in figure 13. The groupings correspond to the mountains on whose slopes they are installed. All sensors on Sukkertoppen lie in the Sukkertoppen grid box. The sensors on the slope of Platå mountain are both in the Huset grid box. And the sensors on Gruvefjellet's slope are both in the Nybyen grid box.

In a less naive approach, using information from more of the surrounding grid points, an interpolation of the model data could be done for each observation location. In this setting such an approach would not be conducive, though. The resolution of the model itself is not able to resolve the varied local topography of side valleys, slopes and cliffs, that defines Longyeardalen on the scale it is supposed to be observed on by the snow depth sensors. The high variability in snow depths on scales even smaller than the side valleys, slopes and cliffs (as

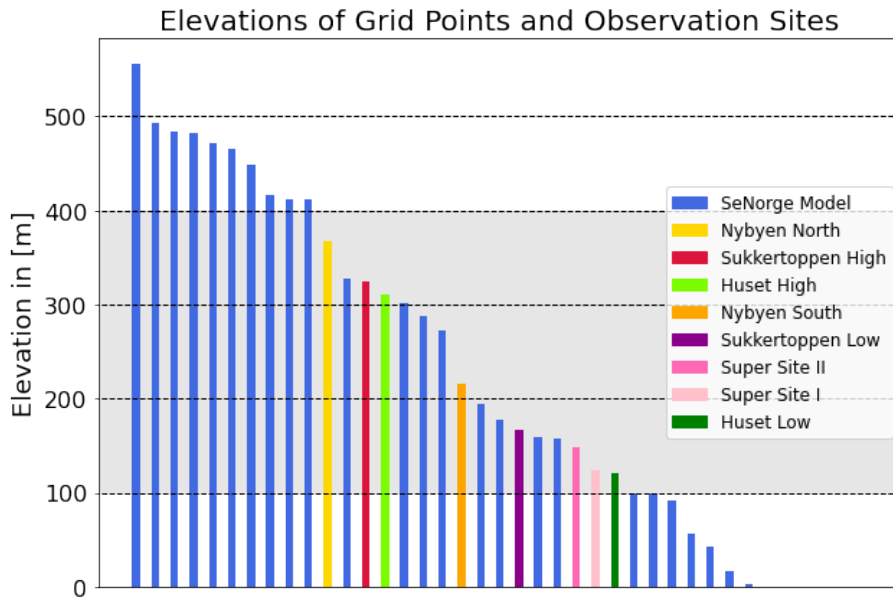


Figure 14: Elevations of SeNorge grid points and observation sites in the area of Longyearbyen as shown in figures 12 or 11. The three comparison sets for elevation collocation (100-199m, 200-299m and 300-399m) are marked with a light grey background.

seen in chapter 2.3.3) adds further to this issue.

The more naive approach of comparing model grid boxes to all the sensors within them is therefore preferable, the hope being that the multitude of sensors will average out the local differences, approaching the model time series in their mean.

It is found that, also within the grid boxes, observation sites are neither numerous nor wide spread enough to enable a meaningful proposition on possible model biases in the three grid boxes studied. The variability between time series of a single grid box matches, or even outstrips, the inter-grid box timeline variability. Using the means of these observed snow depths as benchmarks would introduce large uncertainties. A data set of statistical size, with longer time series and far greater observation site frequency, would be needed. This is impossible with the currently employed observation method.

Elevation Collocation Approach

Analysis of spatial distributions does not have to map snow depths to their horizontal position. Spatial distributions can also refer to vertical distributions, mapping snow depths to their positions in elevation. An elevation dependency in snow depth will show in similar snow depths for sites and grid points of similar elevation. Elevation dependency is a reasonable hypothesis, as precipitation often

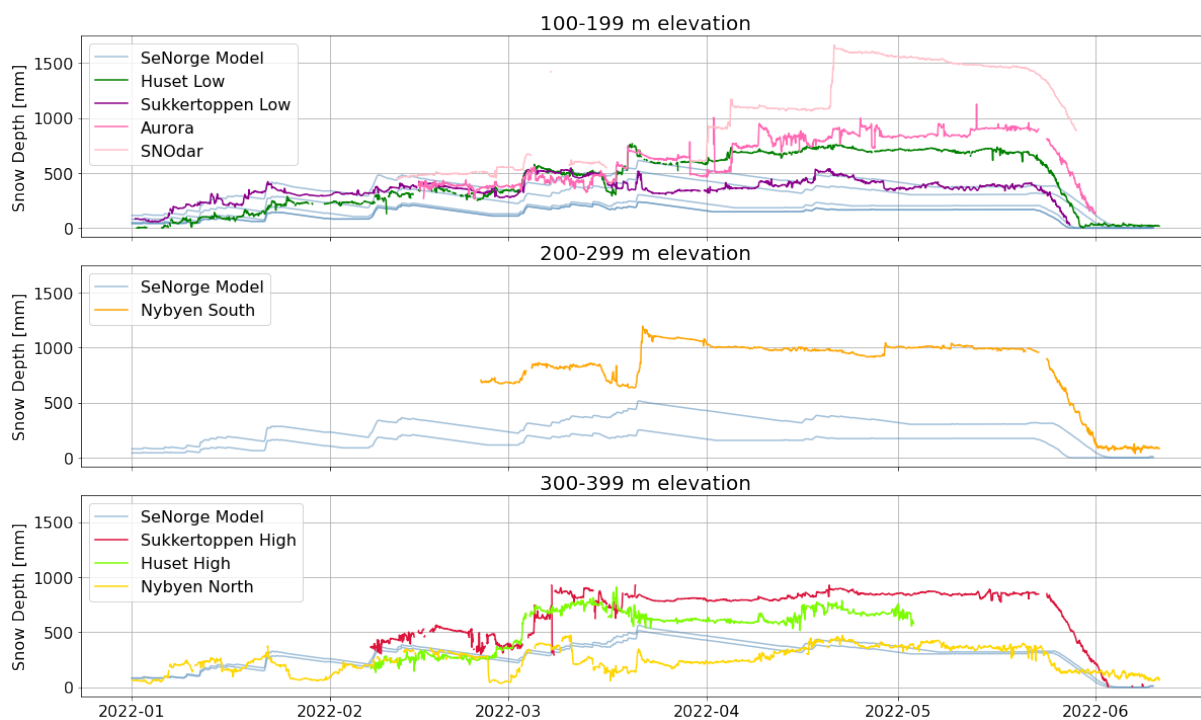


Figure 15: Observed snow depths compared to SeNorge snow depths of similar elevation.

correlates positively with elevation (see chapter 3.2.1). But, when comparing the elevations used by SeNorge for the Longyearbyen area (figure 12) and the snow depths modelled for that area by SeNorge (figure 11), no elevation dependency is apparent. Is this a shortcoming of the model? Do observations favor the hypothesis of elevation dependency?

According to the height distribution of the observation sites, as seen in figure 14, height bins of 100m bin width were chosen to compare model and observation by elevation. This results in groupings of the time series as seen in figure 15. Again, the meaningfulness of the comparison is limited by the scarcity of observation sites and the scale of variability within each bin. No obvious conjoint behaviour of time series in an elevation bin can be observed, though the general magnitude and the timing of increase and decrease is represented. The time series of any elevation bin do not show distinctly different behaviour from those of any other.

Nevertheless, drawing from a study area larger than just the Longyearbyen area, a partial elevation dependency in SeNorge is still probable (see chapter 3.2.1).

3.2.3 *Comparison with Observations in the Temporal Dimension*

In the above analysis of spatial distributions, the comparison of the SeNorge model and the snow depth observations did not prove very helpful. This is mainly due to a discrepancy of scales of interest, the model being designed for regional purposes, the observation network being designed for the monitoring of single slopes. But, in terms of time scales, model and observation time series correspond well. Common features of the evolution of snow depth on the scale of days are targeted by both observation and model representation.

SeNorge's temporal resolution is well capable of reproducing the observed changes in snow depth and features in snow depth evolution. When looking at the time series of the different observation sites and grid boxes, as in figure 13, changes in the snow depth, on the whole, seem to evolve gradually. Certain events, such as the arrival of the snow drift beneath the SNOdar sensor on the super site or the release of an avalanche, may take place suddenly. But such sudden mass movements would pose problems for detection only if they occurred with greater frequency than the 3h time resolution of SeNorge. And, in fact, they were exceedingly rare during the study period. Of course, processes on smaller time scales within the input data of the model might still contribute to the estrangement of model and observation time series, especially when integrated over the full study period.

Problems connected to collapsing the spatial dimensions

A projection onto (a more constrained perspective on) the temporal dimension is achieved by collapsing the spatial dimension. But how to do this? A representative spatial average would be best. But there are several hurdles to this.

As mentioned before, the locations for the snow depth observations were not chosen as representatives of the entire Longyearbyen area. While the model grid points represent the entire area, the observations represent only the avalanche terrain on the steep slopes of the valley. It might not be surprising therefore, that the model consistently underestimates the absolute snow depths when using the observations as a benchmark (even when excluding the two observation sites with highest snow depths! see below).

The frequent measuring gaps in the observation data are also a problem. Averaging over all available sites will produce artificial leaps in the line of the time series where one observation time series stops or picks up again.

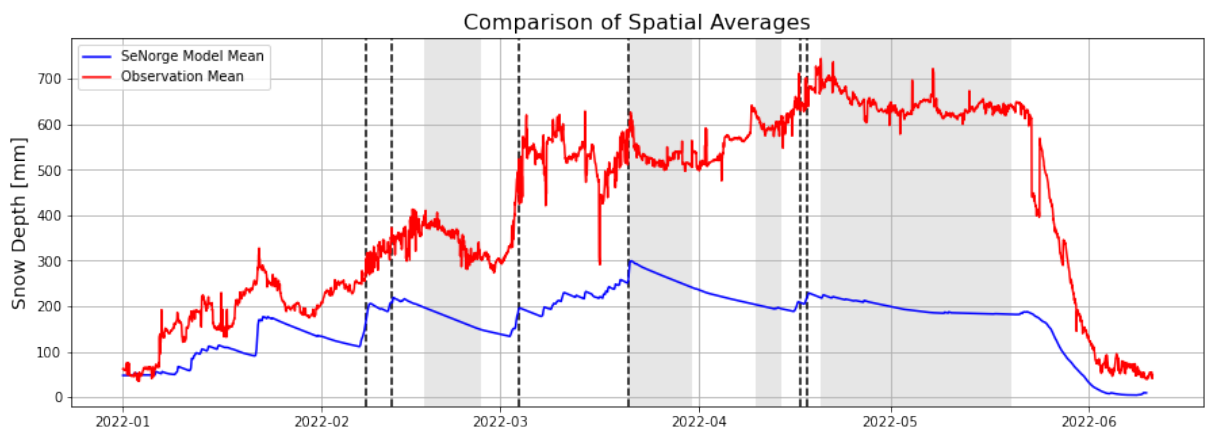


Figure 16: Snow depths compared to SeNorge snow depths averaged spatially over the Longyearbyen area. Measurements from Nybyen South and the SNOdar at the super site were excluded from the mean, as they had large measuringt gaps. Vertical dashed lines signify events with increase in both model and observation. Light grey boxes signify time periods with simultaneous decrease in model and observation.

In this study it was decided to use a very simple average over most available observations, despite the distortions introduced by the above problems (seen in figure 16). It must be stressed that the resulting mean observation time series does not represent the true snow depths of the area. The absolute snow depth values presented by it need not be regionally representative, as it will overestimate the mean snow depths due to the placement of the sensors in avalanche terrain. An analysis of its variations must always be careful of the effects of measuring gaps in the data. It is to be used only as a reference for the moments and durations of time series features.

To minimize the effects of measuring gaps in the individual observation data, the observation average used does not include the measurements from the SNOdar on the super site or from Nybyen South. Their measurement gaps had the greatest effect on the seasonal snow depth evolution, due to the fact that they missed out on the earlier months, when the snow was still less deep, while contributing greatly to the higher snow depths in later months because they were the two sites with the highest general snow depths. Including them in the mean would exacerbate the increase in snow depths in spring artificially. Smaller measurement gaps in most of the remaining sites still distort the signal.

Results for Temporal Comparison

Joint behaviour of the averaged observation's and the averaged model's time series can be analysed in terms of correlation and forecasting skill. Choosing the averaged observations as a reference, the ability of the model to predict this

observational reference can be assessed in a skill score. The skill score compares the forecasting ability of the model to the forecasting skill of a simple reference forecast and is defined as

$$s = 1 - \frac{MSE_m}{MSE_r}, \quad (9)$$

with MSE_m the mean squared error of the model from the observation and MSE_r the mean squared error of the reference forecast from the observation. In this case the observation average was chosen as a reference forecast, such that

$$MSE_m = \frac{1}{n} \sum_{i=1}^n (m_i - o_i)^2 \quad (10)$$

and

$$MSE_r = \frac{1}{n} \sum_{i=1}^n (\bar{o} - o_i)^2 \quad (11)$$

with n the number of time steps in the time series, m_i the values in model time series, o_i the values in observation time series and \bar{o} the mean of the observation time series.

The skill score was found to be -1.09 . The negative number indicates that the model is worse at predicting the observational time series than the simple constant mean over the observational time series. A Murphy-Epstein-decomposition [25] can be applied to the skill score in order to identify the reasons for this bad forecast ability. According to the Murphy-Epstein-decomposition, the skill score falls into three summands, the squared correlation coefficient, the conditional bias from the standard deviations of model and observation and the unconditional bias between the means of model and observation:

$$s = (corr_{mo})^2 - \left(corr_{mo} - \frac{STD_m}{STD_o} \right)^2 - \left(\bar{m} - \bar{o} \right)^2 \quad (12)$$

with $corr_{mo}$ the Pearson correlation of model and observation time series, STD_o and STD_m the standard deviations of observation and model time series and \bar{o} and \bar{m} the means of the observation and model time series. The squared correlation coefficient is an indicator of linear association between the two time series. The conditional bias quantifies the degree of deviation caused by the standard deviations of model and observation. And the unconditional bias is a measure of

deviation between the means of the two time series.

In this case the squared correlation coefficient was 0.67, the conditional bias was -0.23 and the unconditional bias was -1.52 . This implies a fairly good correlation of the two time series, but with a considerable offset in absolute value, caused by the high unconditional bias. This is in line with previous cautioning on using the absolute observation values as a benchmark.

Certain features in the joint behaviour of model and observation time series are best detected visually in the simple comparison done in figure 16.

Increases in snow depth can be seen in both model and observation for several separate events (vertical dashed black lines in figure 16), all of which, notably, were associated to a low pressure system southwest of Svalbard in AROME Arctic reanalysis data. These are presumably precipitation events with mild or no wind influence. While the onset of the increase matches for model and observation, however, the amount of increase varies. If this signal is genuine and not a residual of the observation processing (and careful comparison to the separate time series implies that it is, in fact, genuine), this indicates dependencies of the snow depth difference not included in the model.

The time period and rate of the melting in the beginning of summer correspond well for observations and model. Also, during the snow season itself there are several stretches of gradual decrease in snow depth where slopes match for model and observation (light grey boxes in figure 16). Here, it seems, SeNorge correctly estimates compaction and melting of the the snow pack, while wind transport remains negligible.

3.3 DISCUSSION AND SUMMARY

This chapter concentrated mostly on the first research question. It asked how well the SeNorge snow model for Svalbard represents the spatial and temporal variation of the snow depth distribution.

The comparison of the modelled spatial snow depth distribution and the observed spatial snow depth distribution inherited all the representation problems of the observations described in the previous chapter (chapter 2). This prominently includes the fact that the observations were designed to monitor the slopes of Longyeardalen, not to represent the snow distribution in the Longyearbyen area or make a meaningful interpolation between observation sites possible. The Svalbard SeNorge model, on the other hand, was designed to represent the snow

depth distribution and evolution in Svalbard (albeit not on a local level).

It is therefore unsurprising that, though the general magnitudes of observed and modelled snow depths agree, no good accordance between the absolute values of the observed and modelled snow depths was found on a grid cell to grid cell level. Without a benchmark for comparison to the true snow depth distribution, which the snow depth observations cannot provide, a verification of the spatial distributions given by the model for the Longyearbyen area must wait.

The SeNorge model does not show elevation dependency on the local Longyearbyen scale. However, on a regional scale, effects of orographic precipitation are visible.

The timing of events and features in the temporal evolution of the snow depth are well captured by the model. The absolute values and amplitude of changes varies, though this is difficult to separate from residuals from the processing of the observation data. This variation of absolute change and amplitude is not always represented in the model.

This chapter has also already tapped into the second research question. Elevation was considered shortly as a factor controlling the snow depth distribution. Though it can not be viewed as a meteorological proxy, it has shown itself as a useful measure for snow depth distribution estimates on larger scales. Also, the absolute value and amplitude variations in the time series's features can and will be used in following chapters to separate wind transport effects from precipitation and temperature effects.

SNOWFALL

It is very intuitive to assume a tight correspondence between the amount of snow that falls from the sky and the amount of snow accumulating on the ground (when ignoring melt, sublimation or horizontal divergence). This chapter is concerned with finding that correspondence and establishing whether precipitation can serve as a proxy for snow depth changes. In order to do so, the systematic errors of precipitation observations mentioned in chapter 1.4 need first be accounted for.

4.1 SETUP AND INSTRUMENTATION

4.1.1 *Setup*

Around Longyearbyen precipitation is measured at the three Met Norway weather stations at the airport, on Platå mountain and in Adventdalen (locations as in figure 2 or table 2). The airport and Adventdalen stations use Geonor T-200B all-weather precipitation gauges. The Platå station uses a Thies Clima Laser Precipitation Monitor. Next to precipitation, also snow depth (with a lidar), temperature (with a PT100 sensor) and wind (with a Young 5103 anemometer) are measured.

The main study period is again 01.01.2022 to 10.06.2022. In parts, however, a longer time series was chosen to improve the representativeness of the findings. This was easily possible for the Platå mountain site and the Adventdalen site, where both precipitation and snow depth data has been available for many years (the snow depth measurements are discontinued during summer though). The data used for these sites reaches from the 01.01.2018 to 10.06.2022. For the airport site precipitation data reaches from 21.06.2021 to 10.06.2022, snow depth data reaches from 12.11.2021 to 10.06.2022. For both properties measuring gaps exist in the beginnings of their measuring period. All data is used in hourly resolution here.



Figure 17: Photo of parts of the weather station at the airport. Precipitation gauge on the left, temperature/humidity sensor and snow depth sensor on the right.

4.1.2 Precipitation Gauges

The precipitation gauges at the airport and in Adventdalen are of the type *Geonor T-200B all Weather Precipitation Gauge*. These gauges are the standard for precipitation measurements from Met Norway. They have a wind shield skirt, use antifreeze chemicals instead of an electric heating and a thin layer of oil within the gauge to prevent evaporation loss. The weight of the precipitation accumulated in the gauge during the logging interval is measured with a vibrating wire load sensor, which makes use of the change in natural frequency with applied tension. The shape of the gauge is not ideal considering aerodynamical blockage (shape 1 in figure 18). The precipitation measurements are post-processed for presence of precipitation, which is measured with an additional binary sensor.

4.1.3 Optical Distrometer

The precipitation observations on Platå mountain are taken with a *Thies Clima Laser Precipitation Monitor*. This is an optical distrometer, using a 786 nm laser with max. 0.5 mW power. It scans a measuring area of 23.0 cm by 2.0 cm and classifies the passing hydrometeors by 22 diameter classes (between 0.16 mm and 8 mm) and 20 speed classes (between 0.2 m/s and 20 m/s).

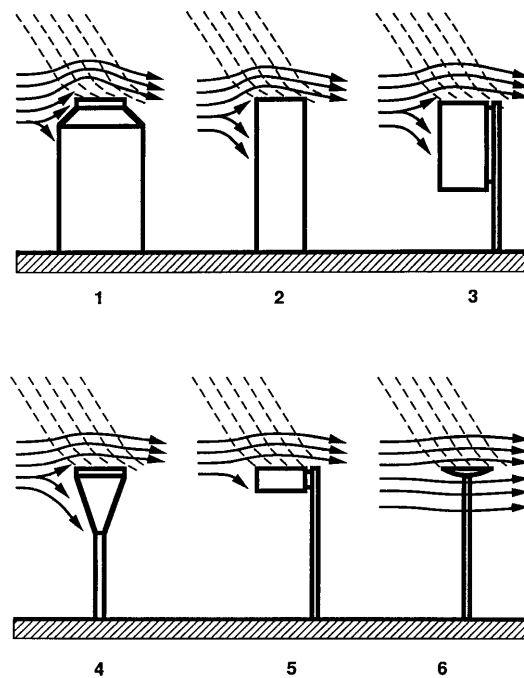


Figure 18: Different shapes of precipitation gauges with respect to undercatch problem. Number 1 indicates the worst performance, number 6 indicates the best performance. Image taken from the WMO solid precipitation measurement intercomparison, 1998 [10].

Compared to precipitation gauges, optical distrometers have several advantages. Wetting and evaporational losses are excluded. Also, aerodynamic disturbance is minimized. Additionally, optical distrometers offer a classification of hydrometeors by type and size. Optical distrometers are not free of measurement bias. Apart from uncertainties derived from the retrieval of the hydrometeor properties, non-precipitation particles may clutter the observation, e. g. from blowing snow, creating systematic error. While standard correction models exist for precipitation gauges, measurement bias in optical distrometers is more difficult to correct for.

4.2 CORRECTION

4.2.1 Undercatch

Undercatch is a classic systematic error. It consists of three loss processes encountered by precipitation measurements with gauges. There is the constant loss of water substance to the walls of the gauge itself. This is called wetting loss. There is the loss of water substance to evaporation. And there is the aerodynamic blockage of the gauge orifice in windy conditions (illustrated in figure 18), which influences both the two previously listed losses and the precipitation entering the

gauge. This aerodynamic factor is especially relevant for solid precipitation.

The magnitude of the undercatch problem is especially pronounced for cold, windy regions such as Svalbard. Here, true solid precipitation is expected to be 1.85 times its measured amount, in seasonal as well as annual average [9]. It is therefore essential to apply a correction model to the measured precipitation data.

4.2.2 Correction Models

The measurements from the precipitation gauges must be corrected for undercatch. Førland and Hanssen-Bauer, 2000 [9] offer a correction formula based on Svalbard's local conditions. It is

$$P_c = k \cdot (P_m + \Delta P_w + \Delta P_e), \quad (13)$$

with P_c the corrected precipitation value, P_m the measured precipitation value, ΔP_w the wetting loss (water substance that is lost to the wetting of the gauges surface) and ΔP_e the evaporation loss. k is a factor for the surrounding weather conditions. For solid precipitation it depends on temperature, T in °C, and wind speed, v in $\frac{m}{s}$, as follows:

$$k = \begin{cases} \exp(\beta_0 + \beta_1 v + \beta_2 T + \beta_3 v T) & \text{for } 1 \frac{m}{s} < v < 7 \frac{m}{s} \\ 1 & \text{for } v \leq 1 \frac{m}{s}. \end{cases} \quad (14)$$

For liquid precipitation $k = \exp(\beta_0 + \beta_1 v + \beta_2 \ln I + \beta_3 v \ln I)$, with I the rain intensity. For mixed precipitation with known liquid-solid ratio, k is expected to be the associated linear combination of k for solid and k for liquid precipitation.

The coefficients ($\beta_0, \dots, \beta_3, \Delta P_w + \Delta P_e$) for equations 13 and 14, taken from Førland and Hanssen-Bauer, 2000 [9], used for the general correction of the precipitation measurements in this study, can be found in table 4. This correction model is compared in figure 19 to a correction model from Rubel and Hantel, 1999 [22], who's coefficients are to be found in table 5.

To apply the correction model to the precipitation data, each event (an hour in which precipitation was measured) must be filtered for the conditions of the model.

Correction Condition Temperature

This includes differentiating between liquid and solid precipitation. Here 0°C was chosen as simple cutoff condition. Precipitation at higher temperatures was

Table 4: Coefficients of correction model from Førland and Hanssen-Bauer, 2000 [9] for Norwegian gauges.

	β_0	β_1	β_2	β_3	$\Delta P_w + \Delta P_e$
solid	-0.04816	0.14883	0.009064	-0,007147	0.10
mixed					0.15
liquid	-0.042303	0.034331	-0.00101	-0.012177	0.15

Table 5: Coefficients of correction model from Rubel and Hantel, 1999 [22] for H&H-90 shielded.

	β_0	β_1	β_2	β_3	$\Delta P_w + \Delta P_e$
solid	-0.0756	0.1100	0.0122	-0.0070	0.08
mixed					0.14
liquid	0.0423	0.0343	-0.0010	-0.0122	0.16

considered to be liquid. Precipitation at lower temperatures was considered to be solid. During the 2022 spring season (01.01.2022 - 10.06.2022) there were 68 such rain events recorded at the Airport Site and 67 recorded at the Adventdalen Site. This corresponds to 28 and 24 percent of precipitation events respectively. Most liquid precipitation fell in the last weeks of the study period, when the snow pack was melting. In the earlier season there was only one occasion with liquid precipitation. There was a warm spell from 14.03.2022 to 17.03.2022, resulting in a rain on snow event. The snow depth decreased by as much as 11cm during the rain on snow event for the airport and Adventdalen sites. For the purpose of this study, cases of liquid precipitation were excluded though, laying a focus on the characteristics of snowfall instead of precipitation in general.

Correction Condition Wind

Another condition of the correction model is a cap on wind speeds for which the correction can still meaningfully be applied. Events with wind speeds $> 7m/s$ must be excluded. From 01.01.2022 to 10.06.2022 22 of the 178 snowfall events recorded at the Airport Site and 71 of the 217 snowfall events recorded at the Adventdalen Site exceeded the wind speed cap and therefor had to be excluded. This corresponds to 12 percent of snowfall events at the airport. But at the generally more windy Adventdalen site 33 percent of all snowfall events had to be discarded. When looking at the extended study period of 01.01.2018 - 10.06.2022, 47 percent of the Adventdalen snowfall events would have to be discarded. This calls into question how sensible it is to measure solid precipitation with a gauge here at all. Does the snow depth change significantly during these strong wind events? Yes, it does. At the Adventdalen site the 71 snowfall events

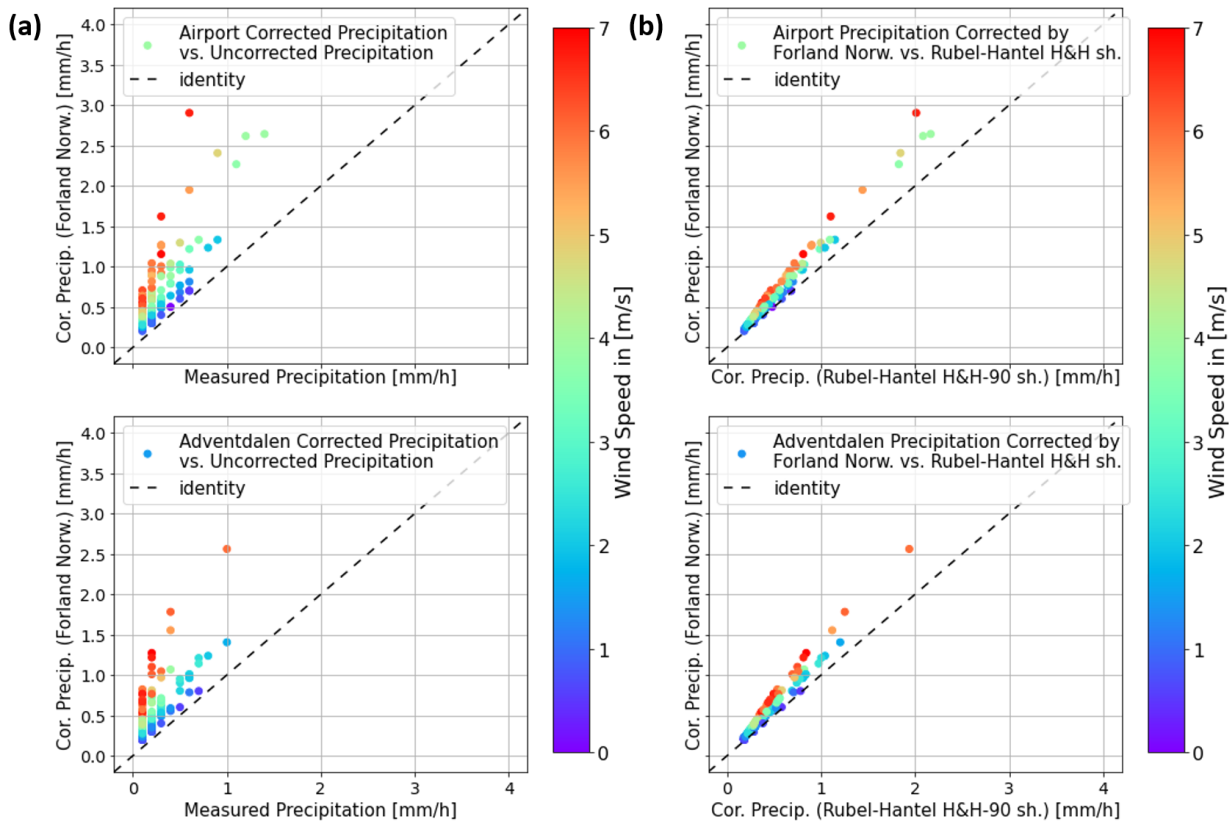


Figure 19: (a) Wind speed (seen in the color dimension) is responsible for the biggest corrections. (b) Where the Førland Hanssen-Bauer model corrects more strongly than the Rubel Hantel model this is accompanied by higher wind speeds. The shown precipitation events are those recorded from 01.01.2018 to 10.06.2022 for the Adventdalen site and from 21.06.2019 to 10.06.2022 for the Airport site.

with winds $> 7\text{m/s}$ account for an accumulated 72.8cm in snow depth difference (hereafter abbreviated as SDD). That's ca. 1cm per event (each event has one hour). The 146 cases with $< 7\text{m/s}$ winds on the other hand account for 60.8cm of accumulated snow depth difference (SDD), which corresponds to only 0.4cm per event. Nevertheless, the following will take into account only the correctable cases. An extra analysis restricted to low wind cases can be found in chapter 4.3.2.

4.3 RESULTS

Precipitation is measured in mm/h of snow water equivalent (SWE). So, to compare precipitation and SDD, the density of the snow pack must be taken into account. Then the equivalent amount of water from the SDD of one hour can be compared directly to the precipitation in that hour. Hourly measurements of snow pack density at the different observation sites is not available. Therefore a simple estimate must be made due with. Snow pack in the Arctic tundra is characterized

by wind slabs and depth hoar, with a typical bulk density of 380 kg/m^3 [26]. This factor is applied in the following when comparing precipitation and SDD.

4.3.1 Results on the Correction Itself

Precipitation and SWE of SDD will be compared directly in the following paragraphs. But first their difference will be used to take a closer look at the applied correction models of precipitation measurements.

When applying the correction to the measured precipitation of the 2022 spring season it becomes obvious (see figure 20) that wind is the main contributor to correction, the wind term being the most pronounced term in almost every event. A good correspondence between magnitude of correction and wind speed can also be seen in figure 19(a), showing a scatterplot of corrected against uncorrected precipitation with wind speed in the color dimension. Each subset of snowfall events of a certain wind speed appears on a separate line. In fact the correction coefficients suggested by Førland and Hanssen-Bauer for Svalbard [9] emphasize wind even more strongly than other correction models, e. g. in Rubel and Hantel, 1999 [22], made for lower latitudes. The correction model for Norwegian gauges in Førland and Hanssen-Bauer, 2000 [9] results in higher snowfall estimates than the correction model for a similar gauge (H&H-90 shielded) in Rubel and Hantel, 1999 [22]. The difference is higher the higher the wind speed is (see figure 19(b)).

Figure 20 shows the different contributions to the correction factor k for environmental influences. The choice of abscissa may seem eccentric at first. It uses the accordance of precipitation and SWE of SDD as an axis. Good accordance,

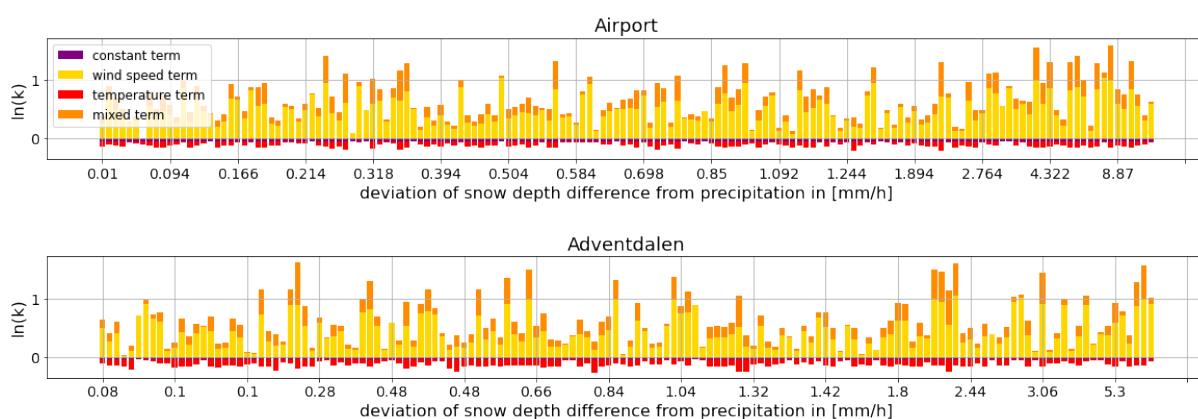


Figure 20: Different terms contribute to the correction factor k . Their respective weights are seen here for each hour of recorded precipitation separately. The events are sorted by the difference between recorded precipitation and difference in snow depth SWE in the same time period. The shown precipitation events are those recorded from 01.01.2022 to 10.06.2022.

resembled by smaller deviations, is found in the left hand part of the plot. Weak accordance, with large deviations, is found in the right hand part of the plot. It was hoped, that this would enable the assignment of the largest deviations to the contribution (or lack thereof) of a certain component of the correction model. This, however, was not the case. Also there is no clear sign, that more subtle corrections (with $\ln k$ closer to 1) are associated to a better accordance between precipitation and SDD.

4.3.2 *Functional Relation between Corrected Precipitation and Snow Depth Difference*

If it is correct that the SDD is mainly dependant on the solid precipitation falling at the time and it is also correct that the snow's density is 380 kg/m^3 , as suggested by Sturm, 1995 [26], then hourly precipitation and hourly SWE of SDD should roughly agree. In figure 21 this would manifest in a tight grouping of data points along the identity line for corrected values. The figure can be respectively interpreted by looking at deviations of possible fits to the data points from the identity, scattering range and, by addition of the wind speed in the color dimension, other likely dependencies such as wind speed.

Functional Fit with Added Density Parameter?

There is no fit for the data points of corrected precipitation obvious to the naked eye. This could imply that precipitation is only one of many parameters shaping the evolution of the snow depth, its signal in the plot thus being disguised. But, when forced into a linear fit through the origin, the lesser slope of the fit when compared to the identity might also point towards a lesser snow pack bulk density (41 kg/m^3 for Plataå, 69.4 kg/m^3 for the airport and 39.2 kg/m^3 for Adventdalen). This density is up to a magnitude smaller than the estimate from Sturm, 1995 [26] and would be small even for freshly fallen snow in calm wind conditions [5]. Despite the fact that the estimate from Sturm, 1995 [26] is a global average, allowing for natural local and timely variation, this seems to be an improbable deviation. However, to be able to distinguish whether the the SDD lacks dependency from precipitation, or whether a different snow pack bulk density would make it possible to explain the shape of the scatter plot with precipitation, direct measurements of the snow pack bulk density at the site would be needed. Such measurements, when carried out regularly, could also help reducing the range in the scattering. Adjusting each point by its own density could nudge the cloud of data points into a more constrained shape. The data points exhibit a significant scattering range. This could be caused by SDD being dependent on other parameters than precipitation, and by the bulk density of the snow pack varying between events.

Functional Fit by Subsets Regarding Wind?

The extra colour dimension was hoped to help find a functional fit for the data points. If distinct subsets of data points were to be seen in the plot (similar to the distinct lines in figure 19), a functional fit might be found for each subset (with constant wind speed) of data points. This would lead to a formula (specific to the study region and period) estimating snow depth differences in dependence of precipitation and wind speed.

The best chance of finding a distinct subset, defined by a certain wind speed interval, for which a functional fit might be found, exists for very low wind speeds. The effects of wind on the precipitation measurements used are strong. A better correspondence between precipitation and SDD might therefore be achieved by limiting the analysis to low wind cases. The cases with wind speeds ≤ 4 m/s are shown in figure 22. But the linear fits forced through the origin are no closer to identity for this subset of cases than for the total of cases. This indicates no improvement of precipitation and SWE of SDD correspondence for limiting to low wind cases.

The majority of data points, however, do seem to follow the line of the identity (especially for uncorrected precipitation). The lesser slope of the fit seems to originate from a slight positive shift in the SWE of SDD as well as a number of outliers with high SWE of SDD and precipitation values. Might the shift towards positive SWE of SDD be a measurement artefact? E. g., might the lidars mistake some part of the falling snow for a surface, thus overestimating the snow depth, especially for larger precipitation intensities?

Figure 21 includes points with negative SDD. From the precipitation point of view (focusing on only precipitation as trigger of snow depth changes) this does not make much sense and might only be explained by measuring or processing errors. The addition of the color dimension helps shed light on the issue, however. In figure 21 negative SWEs of SDDs are often accompanied by high wind speeds. Hence, decreasing snow depth can be said to be coupled with strong winds.

4.4 DISCUSSION AND SUMMARY

This chapter was mainly concerned with investigating precipitation as a possible proxy or predictor of changes in snow depth. To this end a functional relation between snow depth changes and precipitation was sought after. Such a relation could, if found, also be used to fine-tune the correction of the observational bias in precipitation measurements with gauges and also for the distrometer, thus

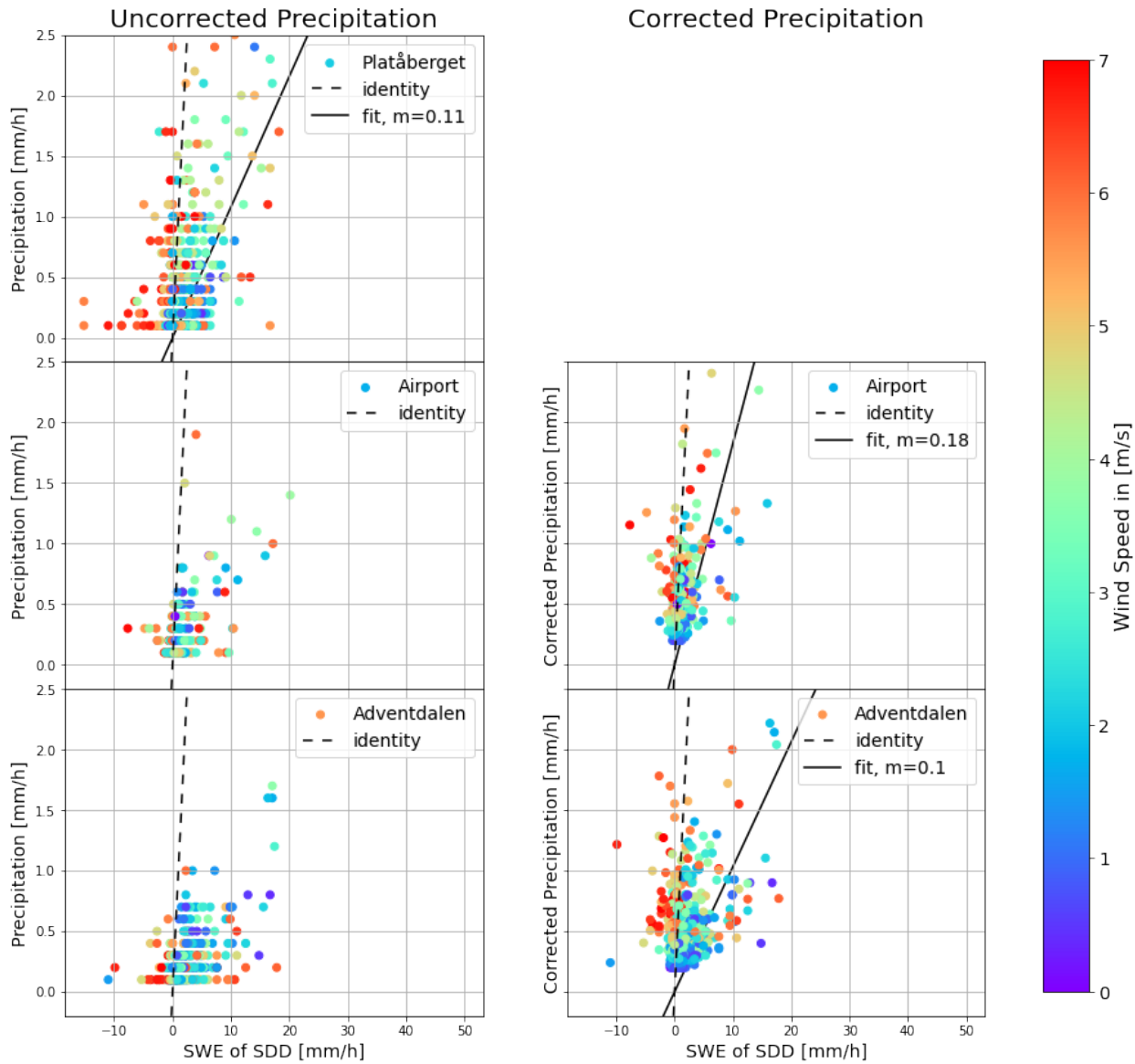


Figure 21: If precipitation were to solely explain the changes in snow depth (and the snow bulk density were a constant 0.38 g/cm^3), all data points would lie on the identity. Wind speed shown in the color dimension. (a) Uncorrected precipitation plotted against the SWE of SDD. (b) Corrected precipitation plotted against the SWE of SDD. Not every data point is shown. Outliers with especially high precipitation values were cut out of the plot to enable a more detailed view of the bulk of data points. The shown precipitation events are those recorded from 01.01.2018 to 10.06.2022.

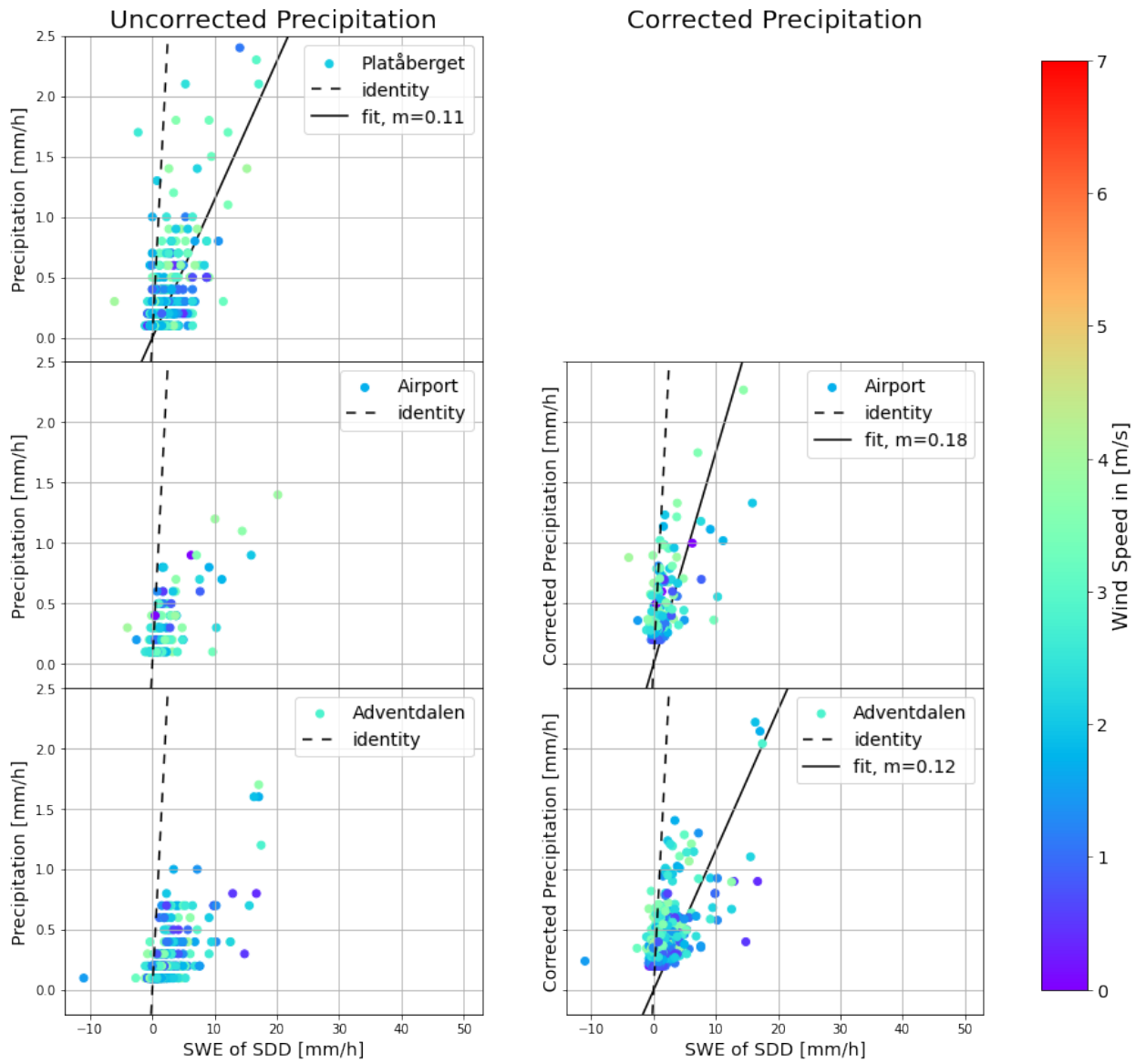


Figure 22: This figure is identical to figure 21, but limited to low wind cases ($v < 4 \frac{m}{s}$).

addressing the last remaining part of the first, more practical research question.

However, no reliable functional fit could be found. Though, as precipitation is probably not the only variable the snow depth changes depends on, functional fits might only exist for subsets of the data points, defined by holding these other relevant parameters at constant values. Snow density and wind speed were considered as such. As no observational data for snow density was taken, a partition by snow density could not be evaluated. For wind speeds, however, the partition of the data set into subsets of high and low wind speeds did not bring the hoped for improvement.

Any conclusive predication as to a functional relation of precipitation and snow depth changes in the area would need a statistical analysis of far greater sample scope. In a data set of sufficient size, significant traits and elements may be found, describing the relation of precipitation and snow depth changes of the area in their mean. Any such elements are too fine to show up to the naked eye, in the data set available in this study, however. It is also far from certain, such statistical elements could provide helpful knowledge in the practical estimation or prediction of snow depths in single events.

Summarizing, in situ precipitation measurements from gauges and distrometers were not found to be a good proxy for snow depth changes in the study area and period.

WIND

From the analysis of the previous chapter it has already become clear, that wind greatly influences the measurement of precipitation. In the previous chapter it has also been shown that negative snow depth differences (SDDs) in the study period and region were mostly accompanied by strong winds ($>5 \frac{\text{m}}{\text{s}}$). This chapter investigates the influence of wind on the SDD in more detail.

5.1 DATA

Snow depth is measured at the Met Norway stations (Platå , Airport and Adventdalen) and at the Longyeardalen sensors (Super Site, Sukkertoppen High/Low, Huset High/Low and Nybyen North/South). The Met Norway sites all include their own wind observations, as does the Super Site.

For the remaining Longyeardalen sensors, which do not have in situ wind measurements, finding a good wind estimate is more difficult. One possibility is using the wind from the nearest Met Norway station (the Super Site wind is highly influenced by the avalanche fence next to which the station is mounted. Hence, it is not a good proxy for the wind at the other Longyeardalen sites).

Another possibility (and the one chosen here) lies with the AROME Arctic weather model¹. The Longyeardalen sensors fall into two grid boxes, one northerly one, encompassing the Sukkertoppen sensors, and one southerly one, including the Huset and Nybyen sensors. In a nearest grid point approach analogous to the one in chapter 3, the modelled 10 m wind at these two grid points of AROME are chosen as reference winds for the anemometerless Longyeardalen sensors.

The winds used for the comparison to snow depth changes are shown in figure 23. The Super Site's wind pattern is clearly influenced by the avalanche fence flanking the Super Site on the south-east. Easterly wind is blocked by it and wind

¹<https://www.met.no/en/projects/The-weather-model-AROME-Arctic>

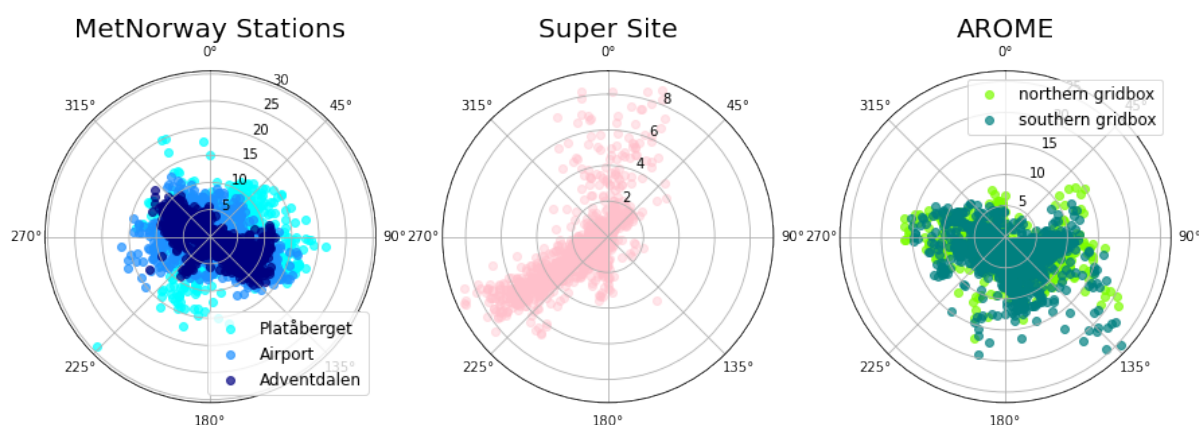


Figure 23: Wind speed and direction from MetNorway stations, super site and AROME model, hourly from 01.01.2022 to 10.06.2022. The super site data has several large measuring gaps.

out of Longyeardalen is channelled alongside it.

There is another data source that is helpful for analyzing the effect of wind on the snow depth. On Gruvefjellet, the plateau mountain on whose slopes the snow depth sensors Nybyen North and Nybyen South are located, there is an automatic weather station (78.1965°N , 15.6326°E , 469m above sea level). It includes a snow drift flux sensor, of the type *FlowCapt Sensor – Model FC4*, mounted ca. 20cm above the ground, and an anemometer, of the type *Young 5103*, mounted at 3m above the ground.

5.2 RESULTS

The momentum of the wind has a considerable effect on the snow pack through the transport of already fallen snow in blowing or drifting snow. In this manner wind blown plateaus are swept clear of snow and cornices form on ridges. It is possible that most snow depth changes observed in the Longyearbyen area arise from wind transport instead of from precipitation.

5.2.1 Snow Depth Changes in Absence of Precipitation

The Met Norway data was categorized for the presence of precipitation, to determine the fraction of SDD not coinciding with precipitation (see table 6). This can then be used to analyze wind-driven changes in the snow depth. Temperatures above freezing were excluded to exclude melting effects.

Times with precipitation show more positive change than negative change, while times without precipitation have similar amounts of positive and negative

Table 6: Snow Depth differences from Met Norway stations hourly data from 01.01.2022 to 10.06.2022, hours with temperatures above freezing excluded.

	total	with precip.	without precip.
positive	835.07 cm	306.96 cm	528.11 cm
negative	804.7 cm	130.61 cm	674.09 cm
total	1639.77 cm	437.57 cm	1202.2 cm

change. As the study period covers an entire season, total positive and negative changes approximately match, as was to be expected. The three Met Norway stations show more snow depth changes for times without precipitation, than for times with precipitation. It may be that most of the snow depth changes are attributed to very small fluctuations in the snow depth observation, not necessarily linked to a physical change in snow depth. This would cause the total SDD in precipitation-free times to exceed the total SDD during precipitation, as times with precipitation are rarer than times without precipitation. However, it is also possible that the small fluctuations in snow depth observations actually document a physical change in snow depth. This change is then most probably an effect of wind transport and compactification.

5.2.2 Wind Speed Threshold for Wind Transport of Snow

Threshold from Conditional Standard Deviation of SDD

Wind transport occurs only above a certain threshold wind speed. When limiting to precipitation-less cases and plotting SDD against wind speed (figure 24), this cutoff appears as the wind speed above which the cloud of data points suddenly expands, at ca. $7 \frac{\text{m}}{\text{s}}$. The conditional standard deviation of the data points, taken for wind speed bins with a width of $1 \frac{\text{m}}{\text{s}}$, increases here. $7 \frac{\text{m}}{\text{s}}$ is a reasonable number when compared to other thresholds found in literature (see e. g. Li, 1997 [16]).

In literature this threshold wind speed has been shown to be related mainly to cohesion and bonding of the particles and their grain size [23], but in Li, 1997 [16] a relation with standard meteorological parameters was sought, using data from the Canadian western prairies. A temperature dependence of the threshold wind speed was found and a formula for the deduction of the threshold wind speed from air temperature was given. Is this consistent with the observations of this study (provided the snow depth changes in absence of precipitation are actually due to physical changes in snow depth triggered by wind transport)? If so, the general pattern of plotting SDD against wind speed should become more

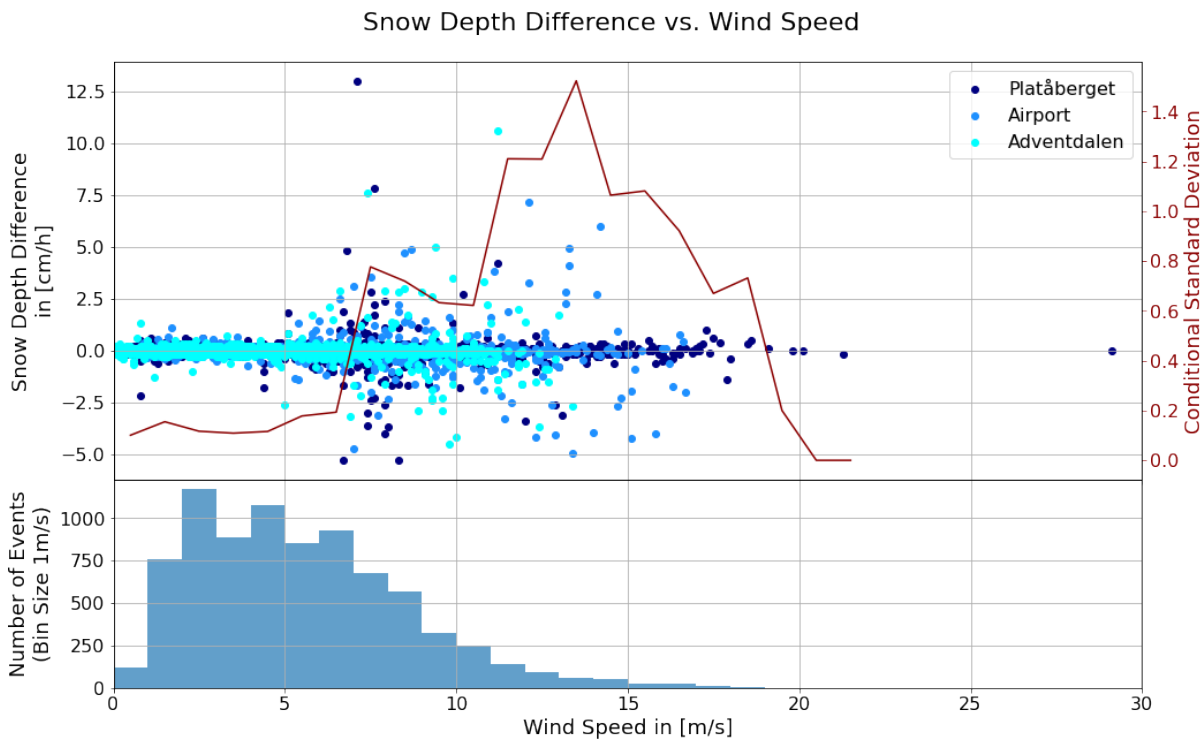


Figure 24: Wind Speed and snow depth difference at the MetNorway stations, when excluding times with precipitation.

clear, when subtracting the threshold deduced from the air temperature from the actual wind speed (see figure 25). A low conditional standard deviation would be expected left of $0 \frac{\text{m}}{\text{s}}$, with a sharp expansion occurring to the right of $0 \frac{\text{m}}{\text{s}}$. In fact, the pattern does not become any more clear to the bare eye (see figure 25). This does not contradict the formula given in Li, 1997 [16] though, which is destined for means of large numbers of events and does not claim to predict the thresholds of single events. It is notable, however, that the expansion point found in figure 25 is shifted slightly from zero to lower wind speeds. This suggests threshold wind speeds generally lower than in Li, 1997 [16]. Here, it may only be guessed at the cause. A possible explanation might be the regional climatic differences between the Canadian western prairies and Svalbard.

Threshold from Flux Measurements

The FlowCapt sensor on Gruvefjellet is concerned with measuring the flux of drifting snow. It consists of a vertical tube with acoustic sensors, mounted between 20 cm and 120 cm above the ground. When the snow depth at the site is less than 20 cm, snow drifting beneath the sensor will be missed. To determine whether this observational bias occurs, snow depth measurements at the site of the flux measurements would be necessary. Also, snow can be blown

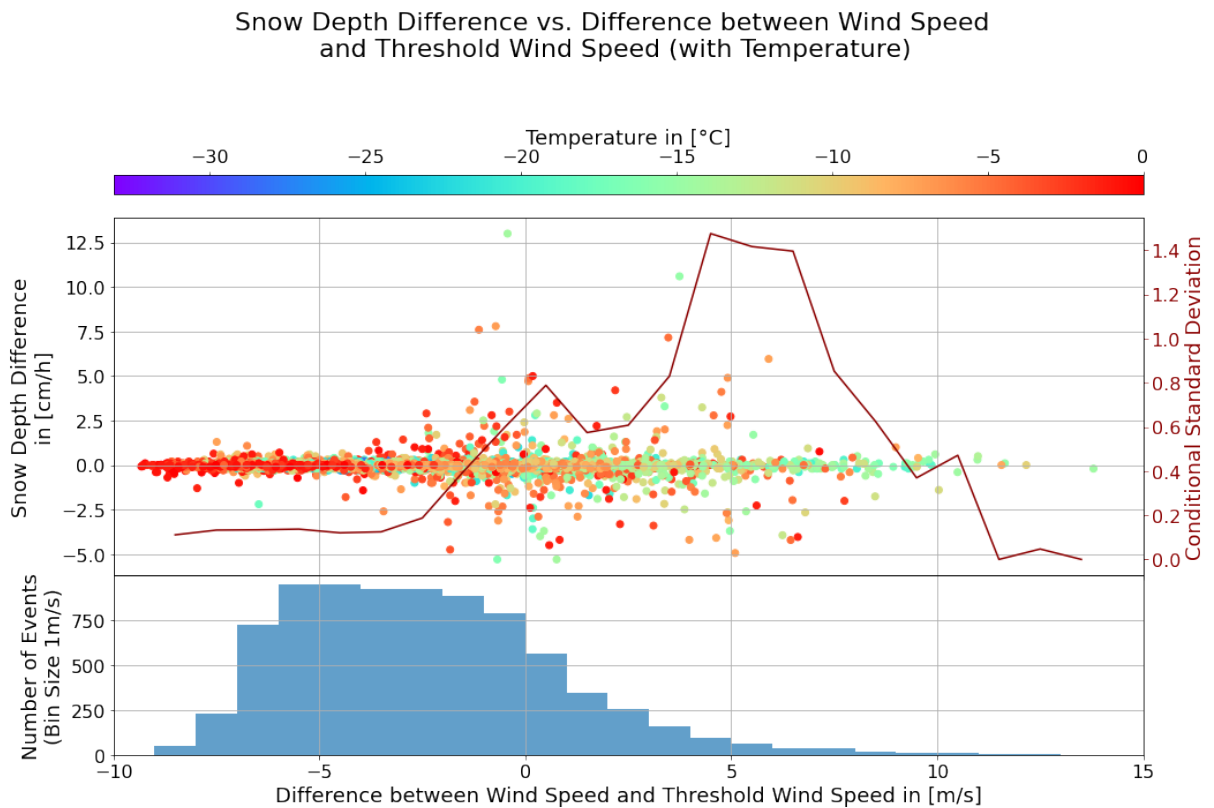


Figure 25: Snow depth at the MetNorway stations plotted against the difference between the actual wind speed and the threshold wind speed deduced from the air temperature as in Li, 1997 [16], when excluding times with precipitation.

above the sensor limit. When neglecting these possible biases, a local wind speed threshold for wind transport of snow can be deduced from the flux measurements.

In a methodology similar to that in Li, 1997 [16], a histogram of wind speeds in events with drifting snow was drawn up (see figure 26). The data set comprises 4446 events. An event, in this data set, is 10 minutes long. These events relate to ca. a month of drifting snow throughout the season in total, but only few events with large quantities of drifting snow.

The shape of the histogram of drifting snow events is determined by two overlying influences. The first of these influences is the distribution of wind speeds independent of the presence of drifting snow (shown in figure 26(a) in the all-time-steps histogram). The second is the threshold of wind transport, which should show up as a pronounced step in the histogram of drifting snow events (also figure 26(a)) and as the wind speed region where the fraction of drifting snow events rises close to one in figure 26(b).

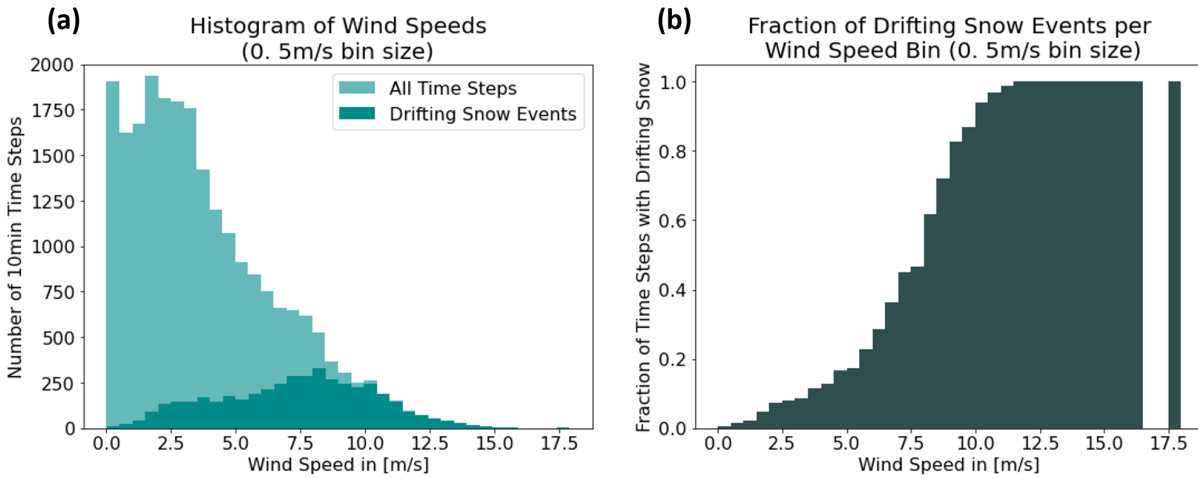


Figure 26: Wind speeds at the weather station on the plateau of Gruvefjellet. Histogram bin size of 0.5 m/s, time step of 10 min. (a) Histograms of all time steps and of those with drifting snow; (b) Fraction of drifting snow events per wind speed bin.

Two modes are apparent in the histogram of drifting snow events of figure 26(a), one close to $2 \frac{\text{m}}{\text{s}}$ and one around $7 \frac{\text{m}}{\text{s}}$. The first mode likely indicates drift of a certain particle type, quicker to be separated out of the snow cover, such as freshly fallen snow. The second mode (at $7 \frac{\text{m}}{\text{s}}$) is thought to be inherited from the distribution of all time step wind speeds, as this exhibits a distinct shoulder, jutting out of the all time steps histogram of figure 26(a) at ca. $7 \frac{\text{m}}{\text{s}}$.

In figure 26(b) the fraction of time steps with drifting snow rapidly rises to one in the region around $7 \frac{\text{m}}{\text{s}}$. Almost all time steps with winds above $11 \frac{\text{m}}{\text{s}}$ record drifting snow.

This sets the boundaries for the wind speed threshold. Wind transport starts at ca. $2 \frac{\text{m}}{\text{s}}$ with snow conditions defined by many vulnerable particles. More types of snow conditions are included with rising winds. And at $11 \frac{\text{m}}{\text{s}}$ all snow conditions are subject to wind transport.

5.2.3 Magnitude of Effect of Wind Transport of Snow

It is difficult to formulate general statements on the magnitude of the effect wind transport has on the snow depth. But several specific points can be drawn from the data of the Gruvefjellet weather station and are listed in the following.

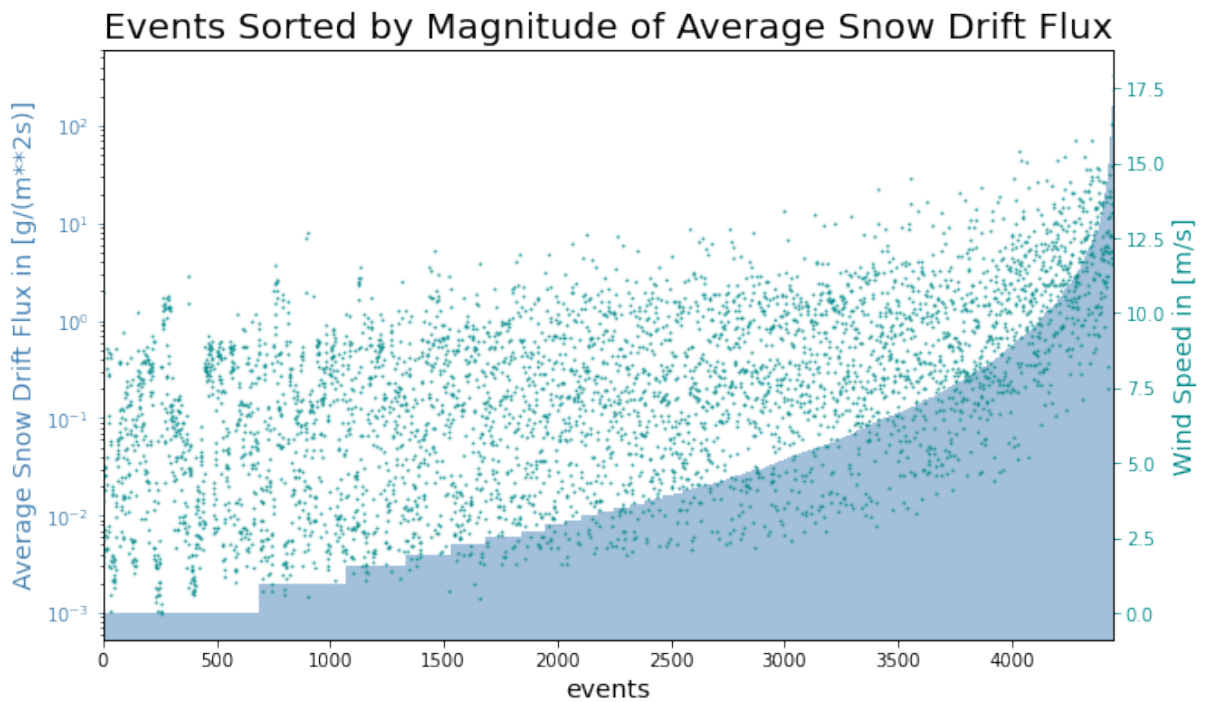


Figure 27: Wind speed is scattered over the mean fluxes of drifting snow sorted by size. A super-exponential increase of flux with increasing wind speeds is visible, though variation is considerable.

Abundance of Drifting Snow Events

Concerning the temporal dissemination of drifting snow, the Gruvefjellet data suggests drifting snow is a fairly common phenomenon (even without the drifting snow possibly lost passing underneath the sensors reach). 4446 10-minute events of drifting snow are recorded from 01.01.2022 to 10.06.2022. This corresponds to a total time of 30.875 days within less than six months, a fraction of ca. 20%.

For wind speeds above $11 \frac{\text{m}}{\text{s}}$ drifting snow is nearly always present.

Magnitude of Flux with Relation to Wind Speed

It can also be said with reasonable certainty that higher wind speeds correspond to higher fluxes of drifting snow. In figure 27 wind speeds and average snow drift fluxes are plotted together. The fluxes are scaled logarithmicly, making a slight super-exponential dependency of snow drift flux from wind speed visible.

Estimation of Amount of Snow Accumulated in Lee

Note: This is only a mind game. The given observations do not constrain the problem well enough for scientific estimates.

The total cumulative flux of drifting snow at Gruvefjellet weather station for 01.01.2022 - 10.06.2022 is $1131.9 \frac{\text{kg}}{\text{m}^2}$. How much of that snow will accumulate at the snow depth sensors in the vicinity?

There are two snow depth measuring sites available close by. Both Nybyen North and Nybyen South are located in the slope falling towards Longyearbyen from the plateau on which the weather station stands. This slope is very steep. In its upper part it is a cliff on whose upper edge cornices form during the snow season. Assume all snow blown over that edge accumulates at the base of the cliff on the slope with the snow depth sensors (this is of course a gross oversimplification).

The wind direction observations from the Gruvefjellet weather station are faulty. Take the wind direction from AROME instead. Limit to cases with wind between 50° and 190° , which are winds from the plateau blowing towards Longyearbyen (see figure 2 as a reference). The total cumulative flux of drifting snow limited to this interval is $165.6 \frac{\text{kg}}{\text{m}^2}$.

A very rough estimation puts the area of this slope to be $700\,000 \text{ m}^2$ and the length of the edge of the plateau to be 900 m . The unit of the flux recorded by the Gruvefjellet station is normalized to represent the flux through a 1m by 1m square, put up at the station. So during the course of the season $900 \times 165.6 \text{ kg}$ of snow is blown from the edge of the plateau into the slope. That makes for an average accumulated snow depth of only 0.0006 m for a general density of 0.38 g/cm^3 , as in Sturm, 1995 [26].

This seems to be a negligible amount. However, apart from the large uncertainties attached to all the simplifications made, there are two factors that might be responsible for falsely lowering this estimate. The slope area on which the snow is distributed may be too large. If the snow were to only accumulate directly beneath the cliff, this would make for an area smaller by at least an order of magnitude. Also, snow blown either underneath, or, in strong wind cases, above the flux sensor could add significantly to the measured fluxes.

5.2.4 *Prevailing Wind Directions*

The direction of the wind is important for the accumulation or depletion of snow because it determines whether the site is in a wind shadow or not. Also, it is important whether there is transportable snow upwind from the site (e. g. for wind coming from the open sea, there is no transportable snow).

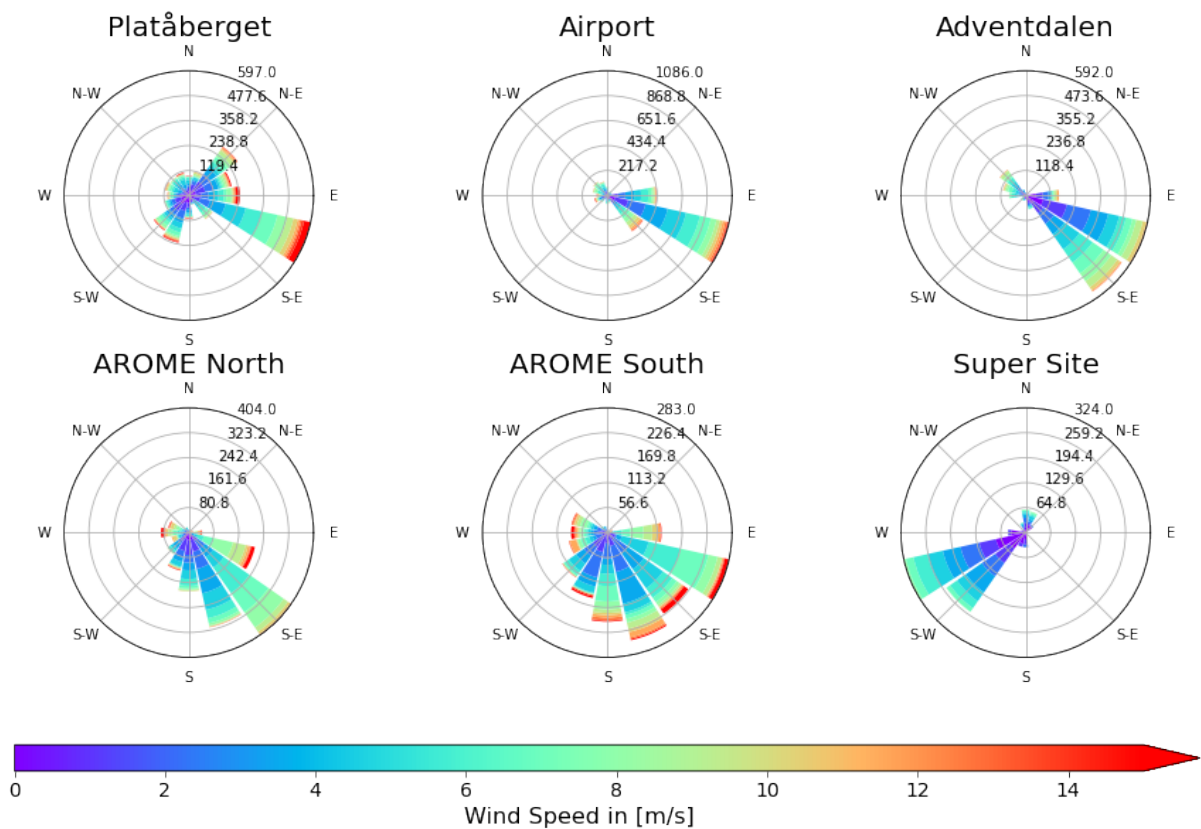


Figure 28: There are certain wind directions typical for certain locations. This can be seen by plotting the number of time steps (1 hr) of a given wind speed for each direction.

To find the prevailing wind directions for each site consider figure 28.

While the Met Norway stations are located in locally flat terrain without direct wind shadow, the direction of the wind can still influence them due to the prevailing flow patterns determined by the regional topography and the upwind sources of transportable snow. All Met Norway stations show the highest frequencies for winds from the southeast. The Platå station is situated at a high altitude and exposed to winds relatively uninfluenced by the local valley topography. Its prevailing flow direction is from east-south-east. But there are also a fair amount of winds from the southwest. The Airport and especially the Adventdalen site are influenced by the main valley direction of Adventdalen and the Adventfjord, which happen to align with the prevailing wind direction measured at the Platå. The Adventdalen site has slightly more southeasterly winds, while the Airport site's winds concentrate around the east-southeast. This might be due to a slight bend in the valley.

The super sites' signal is clearly influenced by the avalanche fence. It alone shows winds predominantly from the southwest. It is possible to track these

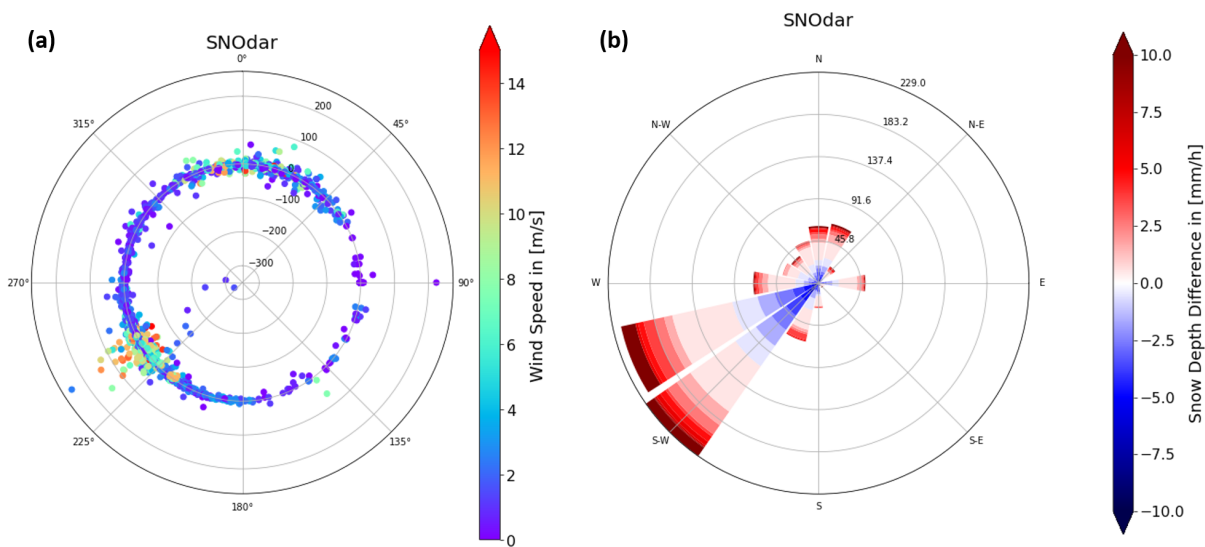


Figure 29: Wind and snow depth beneath SNOdar. A positive SDD-signal can be seen for southwesterlies. This corresponds to the growing of the snow drift discussed in chapter 2.3.3. SDD on radial axis; (a) shows SDD and wind direction of each event with wind speed in the color dimension, (b) shows SDD frequency for each of 16 wind direction bins.

winds to times where the AROME data shows easterly flows. Easterly winds are turned around the fence, which redirects them downhill along its line, also decreasing them in speed.

The 10 m wind from the two AROME grid boxes used here differ slightly from the observed wind at the Met Norway stations (and of course at the super site). The modelled winds from AROME, especially for the southern grid box, have a larger portion of more southerly winds. They also exhibit more variability in the wind direction. Wind speeds are comparable to the observations.

5.2.5 Changes in Snow Depths with Regard to Wind Directions

The wind direction can be linked to typical changes in snow depth per directional bin. This is shown exemplary in the case of the SNOdar in figure 29. Both figure 29(a) and (b) show snow depth changes in mm/h on the radial axis. (a) illustrates wind speed for each event. (b) illustrates frequency of SDD values. Limiting the analysis to the times with existing wind observations, a clear positive SDD signal can be seen for winds from the southwest. This coincides with the growing of the snow drift discussed in chapter 2.3.3.

The same plot is made for all the sensor sites in figures 30 and 31. But, in these, the super site uses the AROME winds, for better comparability to the other

Longyeardalen sites.

In figure 30 (analogous to figure 29(a)), the SDDs of all snow depth measuring sites are plotted with respect to wind direction and wind speed (in color dimension). Where in situ wind measurements are available, it can generally be observed that larger SDDs occur where the wind speed is higher. There are also directions typical for this, e. g. southeast for Adventdalen. This signature is missed for the Longyeardalen sensors. The AROME wind is likely not site-specific enough to show this kind of signature.

In figure 31 (analogous to figure 29(b)) the dimension of the wind speed is dropped in favor of depicting frequency of wind directions. A great difference can be seen in the data from the Met Norway stations and the other sites. The snow depth changes at the Met Norway stations are markedly smaller than those at the other sites. This is probably at least partly due to the location of the sensors. In flat and open terrain, such as at the Met Norway stations, no loading with snow occurs, as it will in steep, avalanche prone terrain. The different instrumentation and post-processing may also play a role, though.

Changes in Longyeardalen Snow Depth with Regard to Wind Direction

In mountainous terrain such as Longyeardalen the wind direction will have great influence over the accumulation or depletion of snow. Sites located in the lee, or wind shadow, of mountains or ridges have a better chance of accumulating the snow blown there. Analysing the Longyeardalen sensors for SDD's dependence on wind direction is hence especially interesting. The problem with this is, of course, the lack of in situ wind measurements for these sites. When contemplating figures 30 and 31 it must be kept in mind, that the wind used is that of the AROME Arctic weather model's nearest grid point.

Huset High, Huset Low, Nybyen North and Nybyen South all use the wind from the southern AROME grid box. The SNOdar, the Aurora, Sukkertoppen High and Sukkertoppen Low all use the wind from the northern AROME grid box. Still, in figure 30 and 31, the wind appears to differ for the sites. This has two reasons. First, the measuring gaps differ for each site. Thus, each site uses its own subset of the common AROME wind data. E. g. while Huset High and Huset Low both use the southern grid box AROME wind, Huset Low has data points for the northeast where Huset High does not. Huset High has measuring gaps for the times with northeasterly wind. Secondly, SDDs for each data point naturally vary from station to station.

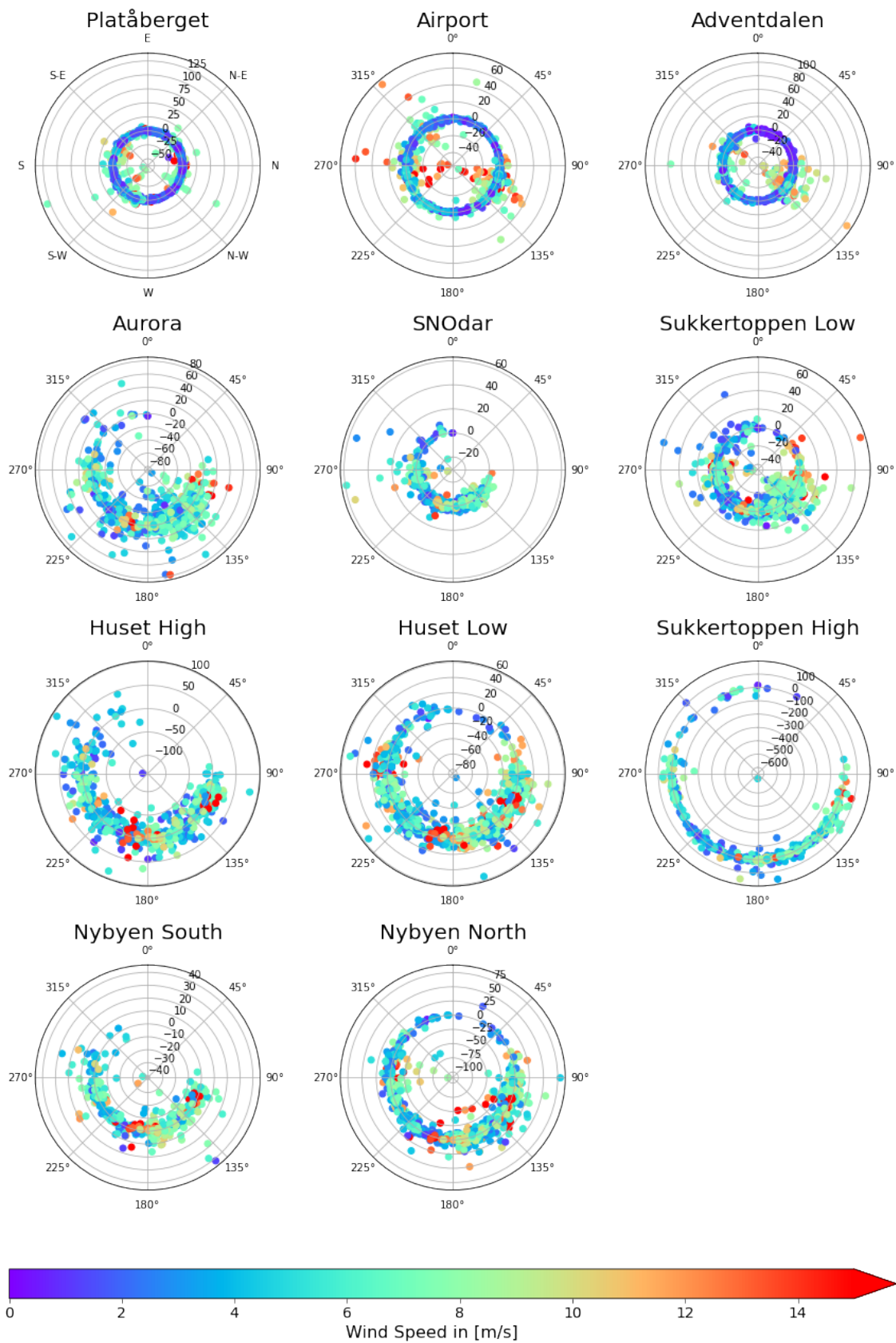


Figure 30: The snow depth change is plotted with respect to the wind direction. Wind speed is seen in the color dimension. For the Met Norway stations in situ wind observations are used. For the sensors on Sukkertoppen (Sukkertoppen High/Low and Super Site) the 10 m AROME wind from the northern grid box was used. For the Gruvefjellet and Plat sensors (Huset High/Low and Nybyen North/South) the 10 m AROME wind from the southern grid box was used.

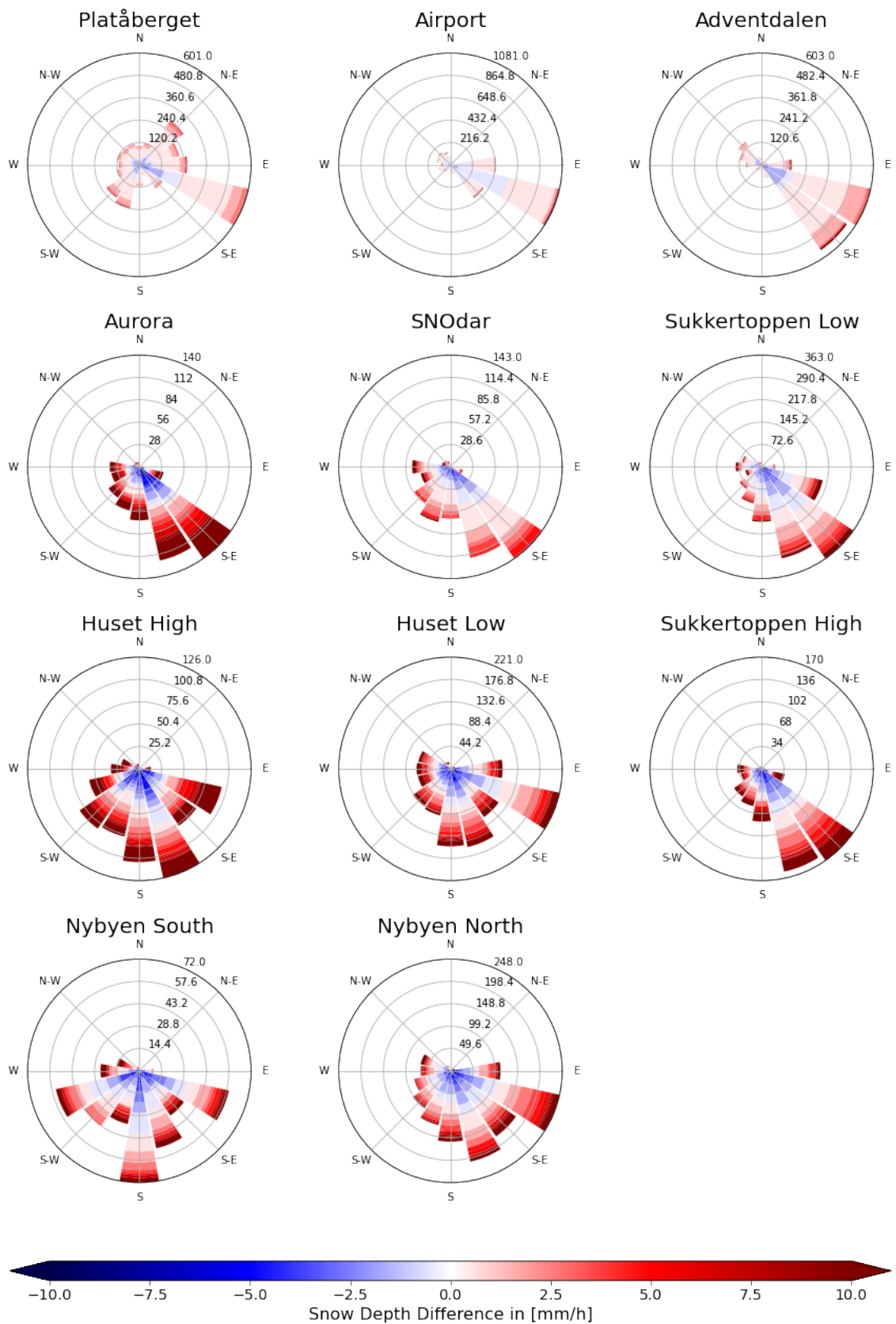


Figure 31: The frequency of different snow depth changes is plotted with respect to the wind direction. For the Met Norway stations in situ wind observations are used. For the sensors on Sukkertoppen (Sukkertoppen High/Low and Super Site) the 10 m AROME wind from the northern grid box was used. For the Gruvefjellet and Plat sensors (Huset High/Low and Nybyen North/South) the 10 m AROME wind from the southern grid box was used.

Table 7: Net snow depth differences depending on luv and lee sides for the Longyeardalen snow depth sensors.

Sites	Lee Interval in [°]	Net SDD in Lee	Net SDD in Luv	Net SDD total
Sukkertoppen High	[160,200]	-914 cm	150 cm	-764 cm
Sukkertoppen Low	[160,200]	-354 cm	146 cm	-208 cm
Aurora	[160,200]	-881 cm	239 cm	-642 cm
SNOdar	[160,200]	-354 cm	146 cm	-208 cm
Huset High	[230,10]	82 cm	179 cm	261 cm
Huset Low	[230,10]	-145 cm	-175 cm	-320 cm
Nybyen North	[50,190]	186 cm	-617 cm	-431 cm
Nybyen South	[50,190]	228 cm	253 cm	481 cm

The portion of negative and positive SDD for each site and wind direction bin were investigated in turn, with the purpose of finding wind directions typical for accumulation or depletion of snow for each site (figure not shown). However, this yields no conclusive signal. Differences between directional bins in the portions of positive and negative SDDs is marginal.

Changes in Longyeardalen Snow Depth with Regard to Luv or Lee

A less detailed view of the Longyeardalen sensors directional patterns should be tried out. The wind directions can be categorized for each sensor as either with the aspect of the slope it is located on, or against it. With the aspect would e. g. mean an easterly wind at a sensor on a slope with easterly aspect, i. e. the sensor would be in the luv of the mountain it is on. When the wind is against the aspect of the slope, this means the sensor is located in the lee.

The portions of positive and negative SDD for this categorization are depicted in table 7 for each of the Longyeardalen sensors. As the total net SDD is very much controlled by the position of measuring gaps in the data, the net luv and net lee SDDs should be considered relative to each other instead of with respect to their absolute values.

The values suggest a relative accumulation of snow on the luv of mountains and a relative depletion of snow on the lee of mountains (except for Huset Low and Nybyen North). This is contrary to what was expected. Relative to the sum of absolute SDD values, however, which range from 50 to 200 m, these net SDDs

are quite small. They might not reflect an actual physical signal so much as a relic from measuring gaps.

5.3 DISCUSSION AND SUMMARY

5.3.1 *Threshold Wind Speed for Snow Transport*

A threshold wind speed for transport of snow was sought after in two different ways. In the snow depth data from the Met Norway stations a threshold was put at ca. $7 \frac{\text{m}}{\text{s}}$ with reference to the divergence of SDD values for wind speeds above this threshold. Attempted validation of an estimation formula for the threshold wind speed in dependence of temperature, which was found in literature [16], showed the threshold wind speed to be slightly lower than predicted. When using data from an automatic weather station on Gruvefjellet including snow drift fluxes, a threshold wind speed between $2 \frac{\text{m}}{\text{s}}$ and $11 \frac{\text{m}}{\text{s}}$ was estimated (likely depending snow conditions).

5.3.2 *Characteristics of Snow Transport*

The Gruvefjellet data suggests that the magnitude of the snow drift flux increases super-exponentially with wind speed.

The flux data from Gruvefjellet can not, however, meaningfully be used to estimate the snow depth on Gruvefjellet's slope, due mainly to too many uncertainties in the snow transfer from the Gruvefjellet station atop the mountain to the snow depth sensors on its slopes (Is the flux at Gruvefjellet station representative for the flux along the entire plateau? How much of the snow reaches the slope? How much of it is carried farther than the slope? What part of the slope does the snow accumulate on?).

High wind speeds were seen to both deplete (Airport) and accumulate snow (super site). For most sites, though, moderate and high wind speeds, while changing the snow depth considerably, have a net zero effect.

5.3.3 *Directional Influence of Wind*

Directional preferences for strong winds (and winds in general) exist for all sites with in situ wind measurements and also for the AROME wind data. South-easterly winds, in particular, are common and often strong. These also coincide with the orientation of Adventdalen, through which the wind is additionally

channeled.

Direction dependency of accumulation or depletion of snow was expected. But no strong signal for this was found, except for the super site with the aforementioned snowdrift creep.

CONCLUSION AND OUTLOOK

This thesis set out to answer the question, what meteorological parameters control the distribution and evolution of the snow depth in the Longyearbyen area. This was done in a fieldwork-based, experimental approach, using in situ data from several weather stations and snow depth measuring sites from the spring snow season of 2022 and modelled weather and snow depth data.

The practical approach implies starting with the exploration of scope and limits of the observations and models that supply the benchmark for any further process-based analysis.

6.1 FIELDWORK AND EXPERIMENTAL RESULTS

6.1.1 *Processing Applied to Observations*

Many of the observations used in this study had to be further processed before using them in the main process-based analysis. A large portion of the work that went into this thesis was put into personal fieldwork hours at the super site and the post-processing of snow depth and precipitation data.

The post-processing of the snow depth observations yielded a first important result for the thesis:

1. The automatic temperature correction in the RXL-MaxSonar-WRS snow depth sensor, used by the DRIVAs and the Aurora, misjudges the air temperature, which is more constant than the internal temperature used for the correction. Reversing the correction eliminates the artificial diurnal cycle introduced by it, yielding a more realistic result. This is not an issue for the SNOdar (radar) or the lidar sensors.

In post-processing the precipitation data, a correction for undercatch was applied for the two sites using precipitation gauges. It was found that

2. wind is the main parameter feeding into the undercatch correction at these sites.

It must, however, be noted that no measure for *true* precipitation, against which the measured and corrected precipitation could be compared, exists at these sites. Snow depth measurements at the sites were also not found to be able to provide this. The correction relies fully on relations found in previous studies and literature.

6.1.2 *Limits of Observations and Model*

After processing the observational data and before looking at the meteorological parameters of precipitation and wind as possible candidates for controlling the snow depth, the ability of the snow depth observations and the snow depth model to represent the snow depth in its spatial and temporal variation was investigated. This was the first research question for the thesis.

It was found that

3. the spatial distribution of snow depths was only poorly represented by observations or model,
4. but the temporal evolution of snow depths was well represented by common signatures in the observation and model time series.

The good temporal representation suggests the existence of crucial (meteorological) processes controlling changes in snow depths across the area. This is promising for the second research question of the thesis (Do precipitation and wind work as proxies for changes in the snow depth?).

The poor spatial representation was put down to the following reasons. In case of the observations:

- (a) The network of snow depth sensors put up around Longyearbyen were not designed or placed for the purpose of representing the spatial distribution of snow in the valley. They were set up as an avalanche risk monitoring system. Accordingly, they were placed only in steep slopes prone to accumulating large amounts of snow and were not equipped with extra sensors for air temperature or snow density, which would have meant additional costs.
- (b) Another problem was the patchy performance of many of the sensors, resulting in frequent and large data gaps and thus making a coherent analysis of mean properties difficult.
- (c) Finally, the large local variability of the spatial snow depth distribution in the Longyearbyen area itself impedes the analysis. As seen in the example of the super site, snow drifts will cause variations in the snow depth in the

magnitude of metres on local scales of metres. This extravagant variability makes a meaningful spatial interpolation of snow depth observations near impossible for any observation network when considering areas as large and varied as the Longyearbyen surroundings.

In the case of the model, a similar reasoning holds true.

- (a) The SeNorge snow depth model was designed to operate on regional scales. Longyeardalen's local topography and the snow depth distribution within it are not resolved by the model.
- (b) It was not possible to bring the modelled snow depth distribution and the pointwise in situ snow depth observations together. The non-representative placing and high local variability of the observations as well as the regional scale of the model made the direct comparison of the two on the scale of the grid cells meaningless.
- (c) The SeNorge snow depth model does not include wind transport of snow between grid boxes. This is a probable cause of deviation in the absolute magnitude of snow depth increase between model and observations.

6.2 PRECIPITATION'S AND WIND'S INFLUENCE ON SNOW DEPTH CHANGES

The second research question for the thesis was to determine the influence of precipitation and wind on changes in the snow depth. This yielded a slightly paradoxical result:

5. Neither precipitation nor wind was found to be a good proxy for changes in snow depth. However, despite of this, both precipitation and wind were found to have a great influence on snow depth changes.

The high variability in snow depths, but also in wind and maybe, to a lesser degree, in precipitation, is inherited by their respective correlations. For any single case or event the predictive authority of precipitation or wind as a proxy is negligible. But in a statistical sense they have a marked influence. This is seen in the following findings.

6. The amount of precipitation was not found to determine the amount of snow depth change.
7. Yet, the timing of precipitation events (when coinciding with calm wind situations) and leaps in the snow depth correspond well. Positive leaps were found for temperatures below freezing. A negative leap was found during the rain on snow event recorded in mid March.

8. Large changes in snow depth (both positive and negative) were mostly accompanied by high wind speeds.
9. Drifting snow was found to be frequent (20% of the time at Gruvefjellet station, with a threshold wind speed of ca. $7\frac{m}{s}$). But it could not be confirmed that the mass flux of drifting snow contributed significantly to the total snow accumulation.
10. The prevailing wind directions were not found to determine the distribution of snow depths. Neither were snow depth observation sites found to accumulate or lose snow according to luv or lee or any other specific wind direction.

6.3 OUTLOOK

Looking back on the work conducted in this study, there may be several approaches worth modifying when repeating a similar analysis. One major hurdle for the analysis of the snow depths in Longyeardalen were the considerable measuring gaps in the data from the Longyeardalen snow depth sensors. Reducing these gaps would improve interpretation of results such as they were found in this study. Also, some additional measurements would be helpful. These include external temperature measurements at sites with sonar snow depth measurement and density measurements at all snow depth measuring sites. Wind emerged from this study as a fascinating factor in snow depth distribution and evolution. To further investigate its impact, additional flux measurement sites for wind transported snow would be valuable. Also, in situ wind measurements at the Longyeardalen snow depth measuring sites would greatly contribute to a meaningful analysis of the conditions under which snow is loaded or depleted on the slopes.

Given time and the resources, a further investigation of the relation between snow depth changes and the meteorological parameters wind and precipitation in the Longyearbyen area by means of a statistical approach (with a widespread, representative set of observation sites) would be interesting. While these relations are too varied and intricate to establish them in a predictive formula on a case to case basis, a statistical approach to wind's and precipitation's influence is likely to yield better understanding of the mean quantitative effect they have on snow depth changes in the Longyearbyen area. This would link given knowledge of the changing of these parameters due to global warming to the actual snow depths on the ground. This, in turn, would benefit not only meteorological research interests but also local stakeholders in Longyearbyen in their assessment of changing avalanche hazards in a changing climate.

BIBLIOGRAPHY

- [1] M. R. Allen and W. J. Ingram. “Constraints on future changes in climate and the hydrologic cycle”. In: *Nature* 419.6903 (Sept. 2002), pp. 224–232. ISSN: 0028-0836. DOI: [10.1038/nature01092](https://doi.org/10.1038/nature01092).
- [2] A. Carrassi et al. “Data assimilation in the geosciences: An overview of methods, issues, and perspectives”. In: *WIREs Climate Change* 9.5 (2018), e535. DOI: <https://doi.org/10.1002/wcc.535>.
- [3] J. Cohen et al. “Divergent consensuses on Arctic amplification influence on midlatitude severe winter weather”. In: *Nature Climate Change* 10 (Jan. 2020), pp. 20–29. DOI: <https://doi.org/10.1038/s41558-019-0662-y>.
- [4] D. Coumou et al. “The influence of Arctic amplification on mid-latitude summer circulation”. In: *Nature Communications* 9 (Aug. 2018). DOI: <https://doi.org/10.1038/s41467-018-05256-8>.
- [5] K. Cuffey and W.S.B. Paterson. “2 - The Transformation of Snow to Ice”. In: *The Physics of Glaciers*. Ed. by W.S.B. PATERSON. 4. Edition. Amsterdam: Pergamon, 2010, p. 12. ISBN: 978-0-08-037944-9. DOI: <https://doi.org/10.1016/B978-0-08-037944-9.50008-X>.
- [6] A. Dobler, E. J. Førland, and K. Isaksen. *Present and future heavy rainfall statistics for Svalbard – Background-report for Climate in Svalbard 2100*. Tech. rep. 3/2019. NCCS, Feb. 2019.
- [7] C. Engås. “Skred i Vei 228”. In: *SVALBARDPOSTEN* (Feb. 21, 2017). URL: <https://www.svalbardposten.no/skred-i-vei-228/154951> (visited on 01/23/2023).
- [8] E. J. Førland et al. “Measured and Modeled Historical Precipitation Trends for Svalbard”. In: *Journal of Hydrometeorology* 21.6 (2020), pp. 1279–1296. DOI: [10.1175/JHM-D-19-0252.1](https://doi.org/10.1175/JHM-D-19-0252.1).
- [9] E.J. Førland and I. Hanssen-Bauer. “Increased Precipitation in the Norwegian Arctic: True or False?” In: *Climatic Change* 4 (Sept. 2000), pp. 485–509. DOI: [10.1023/A:1005613304674](https://doi.org/10.1023/A:1005613304674).
- [10] B. E. Goodison, B. Louie, and D. Yang. “WMO Solid Precipitation Measurement Intercomparison Final Report”. In: 1998.
- [11] B. Hansen et al. “Warmer and wetter winters: Characteristics and implications of an extreme weather event in the High Arctic”. In: *Environmental Research Letters* 9 (Nov. 2014). DOI: [10.1088/1748-9326/9/11/114021](https://doi.org/10.1088/1748-9326/9/11/114021).

- [12] I. Hanssen-Bauer et al. *Climate in Svalbard 2100, a knowledge base for climate adaption*. Tech. rep. 1/2019. Chapters 4.3 and 5.2. NCCS, 2019.
- [13] E. Holdal and R. Andreassen. “Hus flyttet 80 meter av snømasser”. In: *NRK* (Dec. 20, 2015). URL: https://www.nrk.no/tromsogfinnmark/_-hus-flyttet-80-meter-av-snomasser-1.12713840 (visited on 01/23/2023).
- [14] M. Jarraud. “Polar Meteorology. Understanding global impacts. WMO-No. 1013”. In: ISBN 92-63-11013-1 (2007).
- [15] D. Kim and H. M. Kim. “Effect of data assimilation in the Polar WRF with 3DVAR on the prediction of radiation, heat flux, cloud, and near surface atmospheric variables over Svalbard”. In: *Atmospheric Research* 272 (2022), p. 106155. ISSN: 0169-8095. DOI: <https://doi.org/10.1016/j.atmosres.2022.106155>.
- [16] L. Li and J. Pomeroy. “Estimates of Threshold Wind Speeds for Snow Transport Using Meteorological Data”. In: *Journal of Applied Meteorology - J APPL METEOROL* 36 (Mar. 1997), pp. 205–213. DOI: [10.1175/1520-0450\(1997\)036<0205:E0TWSF>2.0.CO;2](https://doi.org/10.1175/1520-0450(1997)036<0205:E0TWSF>2.0.CO;2).
- [17] E. B. Łupikasza and K. Cielecka-Nowak. “Changing Probabilities of Days with Snow and Rain in the Atlantic Sector of the Arctic under the Current Warming Trend”. In: *Journal of Climate* 33.7 (2020), pp. 2509–2532. DOI: [10.1175/JCLI-D-19-0384.1](https://doi.org/10.1175/JCLI-D-19-0384.1).
- [18] G. J. Marshall, R. M. Vignols, and W. G. Rees. “Climate Change in the Kola Peninsula, Arctic Russia, during the Last 50 Years from Meteorological Observations”. In: *Journal of Climate* 29.18 (2016), pp. 6823–6840. DOI: [10.1175/JCLI-D-16-0179.1](https://doi.org/10.1175/JCLI-D-16-0179.1).
- [19] M. McCrystall et al. “New climate models reveal faster and larger increases in Arctic precipitation than previously projected”. In: *Nature Communications* 12 (Nov. 2021). DOI: [10.1038/s41467-021-27031-y](https://doi.org/10.1038/s41467-021-27031-y).
- [20] M. Rantanen et al. “The Arctic has warmed nearly four times faster than the globe since 1979”. In: *Communications Earth and Environment* 3 (Aug. 2022), p. 168. DOI: <https://doi.org/10.1038/s43247-022-00498-3>.
- [21] M. A. Rawlins et al. “Analysis of the Arctic System for Freshwater Cycle Intensification: Observations and Expectations”. In: *Journal of Climate* 23.21 (2010), pp. 5715–5737. DOI: [10.1175/2010JCLI3421.1](https://doi.org/10.1175/2010JCLI3421.1).
- [22] F. Rubel and M. Hantel. “Correction of Daily Rain Gauge Measurements in the Baltic Sea Drainage Basin”. In: *Hydrology Research* 30 (June 1999), pp. 191–208. DOI: [10.2166/nh.1999.0011](https://doi.org/10.2166/nh.1999.0011).

- [23] R. A. Schmidt. "Estimates of threshold windspeed from particle sizes in blowing snow". In: *Cold Regions Science and Technology* 4.3 (1981), pp. 187–193. ISSN: 0165-232X. DOI: [https://doi.org/10.1016/0165-232X\(81\)90003-3](https://doi.org/10.1016/0165-232X(81)90003-3).
- [24] M. C. Serreze and R. G. Barry. "Physical Characteristics and Basic Climatic Features". In: *The Arctic Climate System*. 2nd ed. Cambridge Atmospheric and Space Science Series. Cambridge University Press, 2014, pp. 23–64. DOI: [10.1017/CB09781139583817.005](https://doi.org/10.1017/CB09781139583817.005).
- [25] H. von Storch and F. W. Zwiers. *Statistical Analysis in Climate Research*. Cambridge University Press, 1999, pp. 399–402. DOI: [10.1017/CB09780511612336](https://doi.org/10.1017/CB09780511612336).
- [26] M. Sturm, J. Holmgren, and G. E. Liston. "A Seasonal Snow Cover Classification System for Local to Global Applications". In: *Journal of Climate* 8.5 (1995), pp. 1261–1283. DOI: [10.1175/1520-0442\(1995\)008<1261:ASSCCS>2.0.CO;2](https://doi.org/10.1175/1520-0442(1995)008<1261:ASSCCS>2.0.CO;2).
- [27] D. Vikhamar-Schuler et al. *Evaluation of downscaled reanalysis and observations for Svalbard - Background report for Climate in Svalbard 2100*. Tech. rep. 4/2019. NCCS, Feb. 2019.
- [28] W. Walczowski and J. Piechura. "Influence of the West Spitsbergen Current on the local climate". In: *International Journal of Climatology* 31.7 (2011), pp. 1088–1093. DOI: <https://doi.org/10.1002/joc.2338>.
- [29] S. Wickström et al. "Present Temperature, Precipitation and Rain-on-Snow Climate in Svalbard". In: *Journal of Geophysical Research: Atmospheres* 125 (July 2020). DOI: [10.1029/2019JD032155](https://doi.org/10.1029/2019JD032155).
- [30] H. Ye et al. "Increasing Daily Precipitation Intensity Associated with Warmer Air Temperatures over Northern Eurasia". In: *Journal of Climate* 29 (Nov. 2015), p. 151103140040009. DOI: [10.1175/JCLI-D-14-00771.1](https://doi.org/10.1175/JCLI-D-14-00771.1).

DECLARATION

I hereby certify that this material is my own work, that I used only those sources and resources referred to in the thesis, and that I have identified citations as such.

Longyearbyen, January 31, 2023

A handwritten signature in black ink, appearing to read 'A. Radlwimmer', with a stylized flourish at the end.

Antonia Louise Radlwimmer